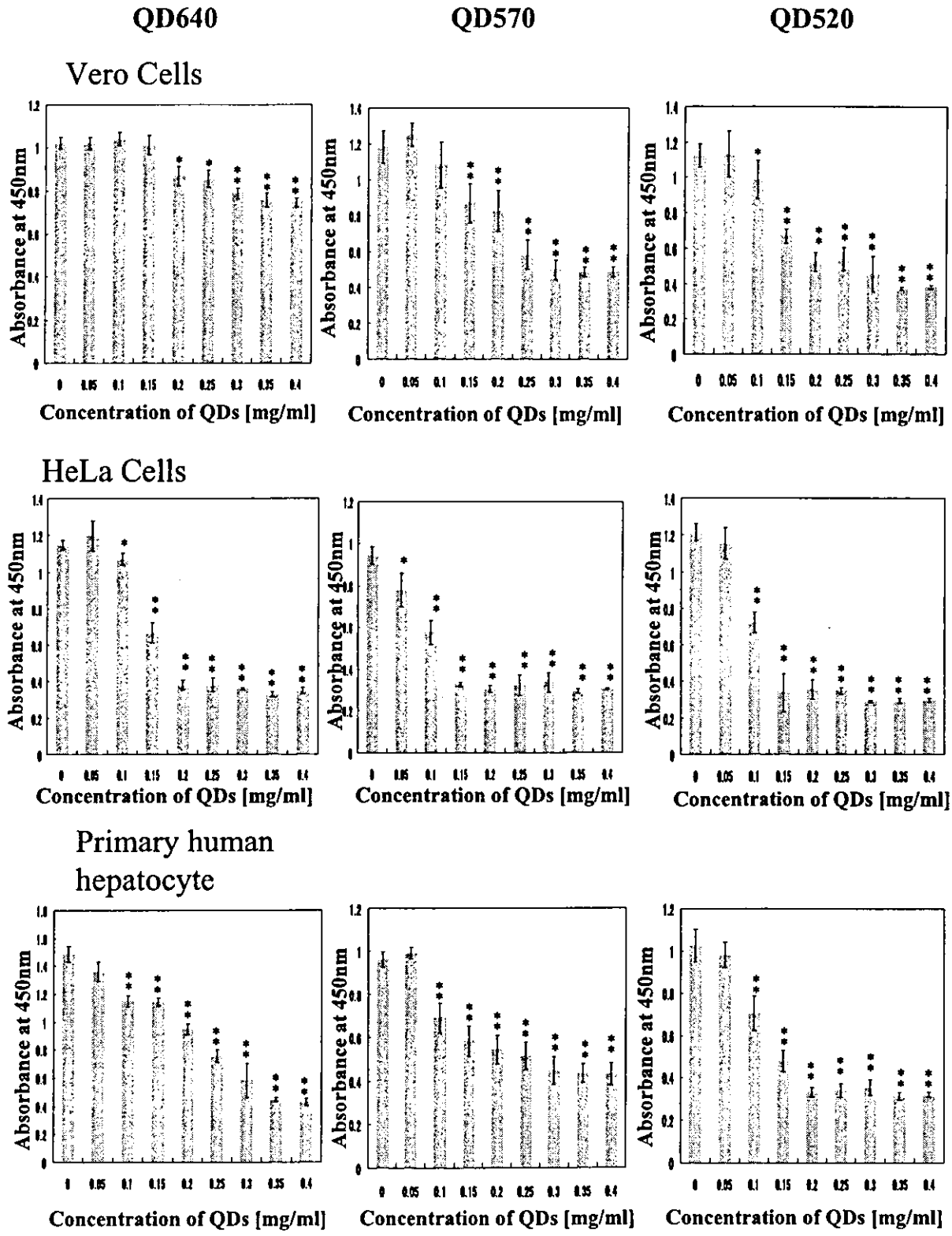

Fig. 2. Cell viability for the different sizes of the QDs and different cell types. Three of the different sizes of QDs are tested on the cell viability for each cell type (MTT assay, $n=5$). The top three panels stand for the cell viabilities of Vero cells, those in the middle for HeLa cells, and those in the bottom for primary human hepatocyte. The three panels in the left lane stand for QD640, those in the middle lane for QD570, and those in the right lane for QD520. In each panel, the horizontal axis stands for the concentration of QD, and the vertical axis stands for the absorbance at 450 nm. The columns in all the panels stand for the amount of hormazan, which reflect the cell viability, and I is standard deviation. A *T*-test was performed; * stands for the significance level <0.01, and ** stands for the significance level <0.001.

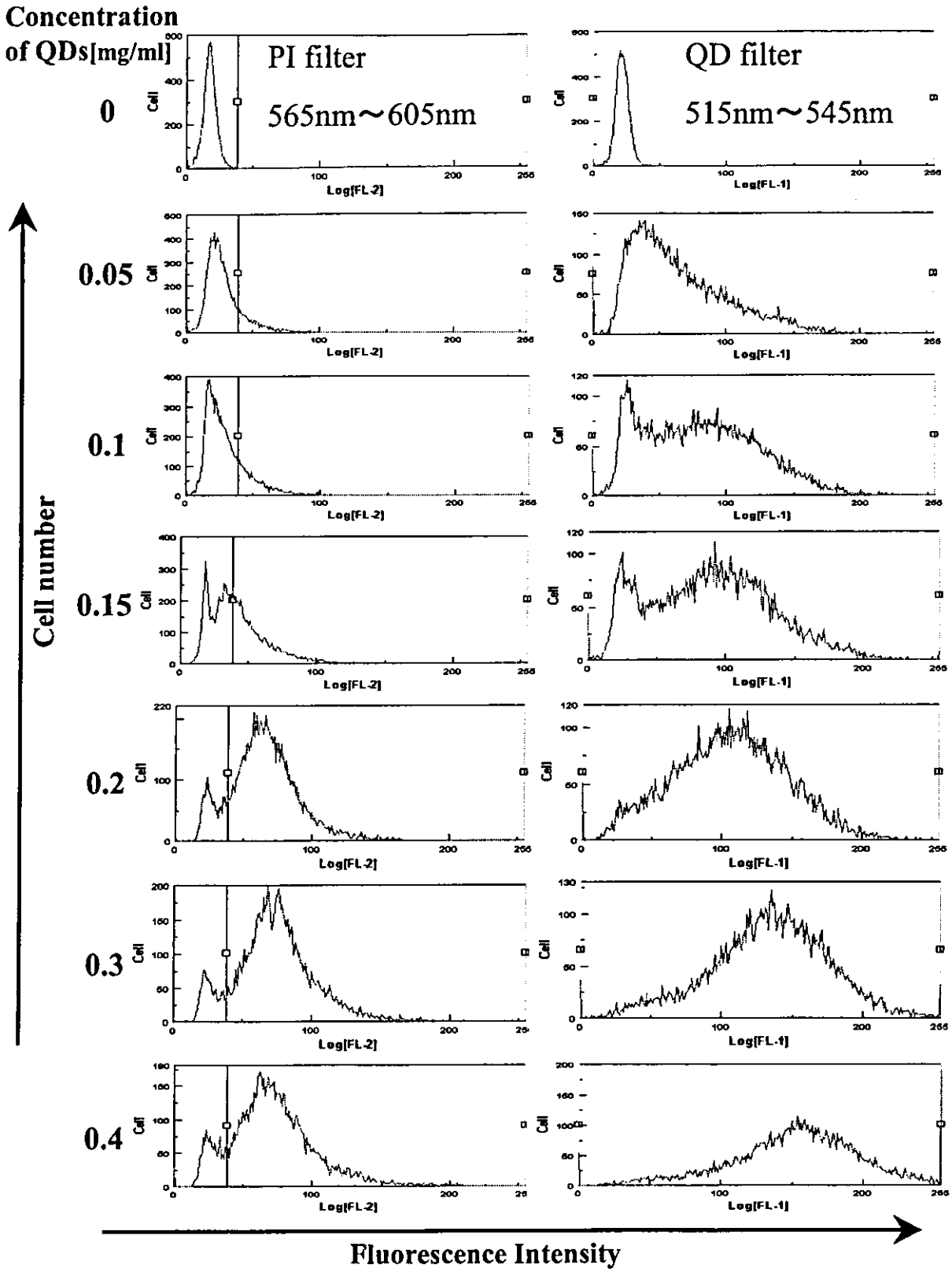

Fig. 3. Flow cytometry assay with the different concentrations of QD. Vero cell and QD520 are used for the flow cytometry assay. The horizontal axis, in the left lane, is the fluorescent intensity of propidium iodide with the filter (565 nm–605 nm), and in the right lane, the fluorescent intensity of QD520 with the filter (515 nm–545 nm). The vertical axes, in both the columns, stand for the cell count. Each row, from the top to the bottom, is given with respect to the concentration of QD520. In each row, the left panel and the right panel show the result with the same sample measured with a PI filter (left) and a QD filter (right), respectively.

QD640. It has been strongly suggested that the mobility of the MUA-QDs inside the cell depends on the size of the MUA-QDs (22). This might also explain the difference in the cell damage in our study.

In order to utilize quantum dots for humans, further study should be done on the relationship between the cell type and MUA-QD cell damage, an estimate of the mutation rate in bacteria and carcinogenesis in animals should be done and research into the mechanism of cyto-toxicity is needed. So far there is currently insufficient information about the discharge of MUA-QDs from living organisms.

We are grateful to Dr. Ohta of Tokyo University of Pharmacy and Life Science for his help with data collection, and proofreading. This work was supported by Grant 'H14-nano-004' of the Ministry of Health, Labour and Welfare of Japan.

References

1) Bruchez, M., Jr., Moronne, M., Gin, P., Weiss, S., and Alivisatos, A.P. 1998. Semiconductor nanocrystals as fluorescent biological labels. Science **281**: 2013–2016.
2) Chan, W.C., and Nie, S. 1998. Quantum dot bioconjugates for ultrasensitive nonisotopic detection. Science **281**: 2016–2018.
3) Coe, S., Woo, W.K., Bawendi, M., and Bulovic, V. 2002. Electroluminescence from single monolayers in molecular organic devices. Nature **420**: 800–803.
4) Collins, A.M., and Donoghue, A.M. 1999. Viability assessment of honey bee, Apis mellifera, sperm using dual fluorescent staining. Theriogenology **51**: 1513–1523.
5) Dabbousi, B.O., Rodriguez-Viejo, J., Mikulec, F.V., Heine, J.R., Mattoussi, H., Ober, R., Jensen, K.F., and Bawendi, M.G. 1997. (CdSe) ZnS core-shell quantum dots: synthesis and characterization of a size series of highly luminescent nanocrystallites. J. Phys. Chem. B **101**: 9463–9475.
6) Dubertret, B., Skourides, D., Norris, J., Noireaux, V., Brivanlou, A.H., and Libchaber, A. 2002. *In vivo* imaging of quantum dots encapsulated in phospholipid micelles. Science **298**: 1759–1762.
7) Elstein, K.H., and Zucker, R.M. 1994. Comparison of cellular and nuclear flow cytometric techniques for discriminating apoptotic subpopulations. J. Neurochem. **74**: 1041–1048.
8) Gerion, D., Pinaud, F., Williams, S.C., Parak, W.J., Zanchet, D., Weiss, S., and Alivisatos, A.P. 2001. Synthesis and properties of biocompatible water-soluble silica-coated CdSe/ZnS semiconductor quantum dots. J. Phys. Chem. B **105**: 8861–8871.
9) Hanaki, K., Momo, A., Oku, T., Komoto, A., Maenosono, S., Yamaguchi, Y., and Yamamoto, K. 2003. Semiconductor quantum dot/albumin complex is a long-life and highly photostable endosome marker. Biochem. Biophys. Res. Commun. **302**: 496–501.
10) Harman, T.C., Taylor, P.J., Walsh, M.P., and LaForge, B.E. 2002. Quantum dot superlattice thermoelectric materials and devices. Science **297**: 2229–2232.
11) Hines, M.A., and Guyot-Sionnest, P. 1996. Synthesis and characterization of strongly luminescing ZnS-capped CdSe nanocrystals. J. Phys. Chem. **100**: 468–471.
12) Ishiyama, M., Miyazono, Y., Sasamoto, K., Ohkura, Y., and Ueno, K. 1997. A highly water-soluble disulfonated tetrazolium salt as achromogenic indicator for NADH as well as cell viability. Talanta **44**: 1299.
13) Kondoh, M., Araragi, S., Sato, K., Higashimoto, M., Takiguchi, M., and Sato, M. 2002. Cadmium induces apoptosis partly via caspase-9 activation in HL-60 cells. Toxicology **170**: 111–117.
14) Kubo, R. 1957. Statistical-mechanical theory of irreversible processes. I. J. Phys. Soc. Jpn. **12**: 570–586.
15) Kubo, R. 1962. Generalized cumulant expansion method. J. Phys. Soc. Jpn. **17**: 1100–1120.
16) Kubo, R. 1962. Stochastic liouville equations. J. Math. Phys. **4**: 174–183.
17) Mosman, T. 1983. Rapid colorimetric assay for cellular growth and survival: application to proliferation and cytotoxicity assays. J. Immunol. Methods **65**: 55–63.
18) Murray, C.B., Norris, D.J., and Bawendi, M.G. 1993. Synthesis and characterization of nearly monodisperse CdE (E=sulfur, selenium, tellurium) semiconductor nanocrystallities. J. Am. Chem. Soc. **155**: 8706–8715.
19) Peng, X., Schlamp, M.C., Kadavanich, A.V., and Alivisatos, A.P. 1997. Epitaxial growth of highly luminescent CdSe/CdS core/shell nanocrystals with photostability and electronic accessibility. J. Am. Chem. Soc. **119**: 7019–7029.
20) Rosenthal, S.J., Tomlison, I., Adkins, E.M., Schroeter, S., Adams, S., Swafford, L., McBride, J., Wang, Y., Defelice, L.J., and Blakely, R.D. 2002. Targeting cell surface receptors with ligand-conjugated nanocrystals. J. Am. Chem. Soc. **124**: 4586–4594.
21) Santori, C., Fattal, D., Vuckovic, J., Solomon, G.S., and Yamamoto, Y. 2002. Indistinguishable photons from a single-photon device. Nature **419**: 594–597.
22) Seydel, C. 2003. Quantum dots get wet. Science **300**: 80–81.
23) Shatrova, A.N., Aksenov, N.D., Poletaev, A.I., and Zenin, V.V. 2003. Effect of etoposide and amsacrine on mitotic progression of GM-130 and Hep-2 cell lines. The flow cytometry assay. Tsitologiia **45**: 59–68.
24) Shen, H.M., Yang, C.F., and Ong, C.N. 1999. Sodium selenite-induced oxidative stress and apoptosis in human hepatoma HepG2 cells. Int. J. Cancer **81**: 820–828.
25) Shubeita, G.T., Sekatskii, S.K., Dietler, G., Potapova, I., Mews, A., and Basch, T. 2003. Scanning near-field optical microscopy using semiconductor nanocrystals as a local fluorescence and fluorescence resonance energy transfer source. J. Microsc. **210**: 274–278.
26) Tominaga, H., Ishiyama, M., Ohseto, F., Sasamoto, K., Hamamoto, T., Suzuki, K., and Watanabe, M. 1999. A water-soluble tetrazolium salt useful for colorimetric cell viability assay. Anal. Commun. **36**: 47.
27) Wu, X., Liu, H., Liu, J., Haley, K.N., Treadway, J.A., Larson, J.P., Ge, N., Peale, F., and Bruchez, M.P. 2002. Immunofluorescent labeling of cancer marker Her2 and other cellular targets with semiconductor quantum dots.

Nat. Biotechnol. **21**: 41–46.

28) Xu, H., Sha, M.Y., Wong, E.Y., Uphoff, J., Xu, Y., Treadway, J.A., Truong, A., O'Brien, E., Asquith, S., Stubbins, M., Spurr, N.K., Lai, E.H., and Mahoney, W. 2003. Multiplexed SNP genotyping using the Qbead system: a quantum dot-encoded microsphere-based assay. Nucleic Acids Res. **31**: 43.

29) Wu, L.X., Steel, D.Y., Gammon, D., Stievater, T.H., Katzer, D.S., Park, D., Piermarocchi, C., and Sham, L.J. 2003. An all-optical quantum gate in a semiconductor quantum dot. Science **301**: 809–811.

30) Zrenner, A., Beham, E., Stufler, S., Findeis, F., Bichler, M., and Abstreiter, G. 2002. Coherent properties of a two-level system based on a quantum-dot photodiode. Nature **418**: 612–614.

Journal of Biomolecular NMR **29**: 543–544, 2004.

Letter to the Editor: ^{1}H, ^{13}C, ^{15}N resonance assignments of the cytokine LECT2

Mie Ito[a], Koji Nagata[a,b], Fumiaki Yumoto[a], Satoshi Yamagoe[c], Kazuo Suzuki[c], Kyoko Adachi[d] & Masaru Tanokura[a,*]

[a]*Department of Applied Biological Chemistry, Graduate School of Agricultural and Life Sciences and* [b]*Biotechnology Research Center, The University of Tokyo, 1-1-1 Yayoi, Bunkyo-ku, Tokyo 113-8657, Japan;* [c]*Department of Bioactive Molecules, National Institute of Health, 1-23-1 Toyama, Shinjuku-ku, Tokyo 162-8640, Japan;* [d]*Marine Biotechnology Institute, Heita, Kamaishi, Iwate 026-0001, Japan*

Received 9 February 2004; Accepted 15 March 2004

Key words: cytokine, LECT2, resonance assignments

Biological context

Human LECT2 (leukocyte cell-derived chemotaxin 2) is a 16-kDa chemotactic protein consisting of 133 amino acids and three intramolecular disulfide bonds. The protein was first purified from the culture fluid of phytohemagglutinin-activated human T-cell leukemia SKW-3 cells as a chemotactic factor to human neutrophils (Yamagoe et al., 1996) and its cDNAs were cloned from cDNA libraries of human, bovine, and murine livers (Yamagoe et al., 1998a,b). LECT2 is identical to chondromodulin-II (Hiraki et al., 1996), a bovine protein that stimulates the proliferation of chondrocytes and osteoblasts (Shukunami et al., 1999). A point mutation in LECT2 (Val58 to Ile58) is associated with the severity of rheumatoid arthritis (RA) (Kameoka et al., 2000). No tertiary structure has been solved so far for LECT2 and its related proteins. In order to reveal the three-dimensional structure of LECT2 and the effect of the point mutation on its conformation, we are doing NMR structural analysis of human LECT2. Here we report the ^{1}H, ^{15}N, and ^{13}C resonance assignments.

Methods and experiments

Human LECT2 (the 133-amino acid mature form, residue numbers 19–151) with an N-terminal His_6-tag was produced in *E. coli* as inclusion bodies, and renatured *in vitro* by a three-step refolding procedure (Ito et al., 2003). To prepare stable isotope-labeled protein, $^{15}NH_4Cl$ (> 99% ^{15}N) and ^{13}C-glucose (> 99% ^{13}C) were used as the sole nitrogen and carbon sources, respectively. The samples used for NMR measurements were 1 mM ^{15}N-labeled and $^{13}C/^{15}N$-labeled $(His)_6$-LECT2 dissolved in 50 mM Na_2SO_4 in 85% H_2O/10% D_2O/5% glycerol (pH 6.0, direct meter reading). NMR spectra were recorded at 298 K on Varian Unity Inova NMR spectrometers operated at ^{1}H frequencies of 500- and 750-MHz and equipped with triple-resonance z-gradient probes.

Sequence-specific backbone assignments were elucidated from 3D data of HN(CO)CA, HNCA, CBCA(CO)NH, HNCACB, CBCANH, HNCO, and (HCA)CO(CA)NH. C(CO)NH was used to confirm amino-acid types. For side-chain ^{1}H assignments, H(CCO)NH, HCCH-TOCSY, HCCH-COSY, ^{15}N-edited TOCSY, ^{15}N-edited NOESY, and 2D NOESY were used. ^{1}H chemical shifts were directly referenced to the resonance of 2,2-dimethyl-2-silapentane-5-sulfonate (DSS), while ^{13}C and ^{15}N chemical shifts were referenced indirectly to DSS (Wishart et al., 1995). NMR data were processed using NMRPipe/NMRDraw (Delaglio et al., 1996). Visualization of transformed data and peak-picking were carried out using Sparky (http://www.cgl.ucsf.edu/home/sparky/). Secondary structure was predicted using CSI (Wishart and Sykes, 1994).

*To whom correspondence should be addressed. E-mail: amtanok@mail.ecc.u-tokyo.ac.jp

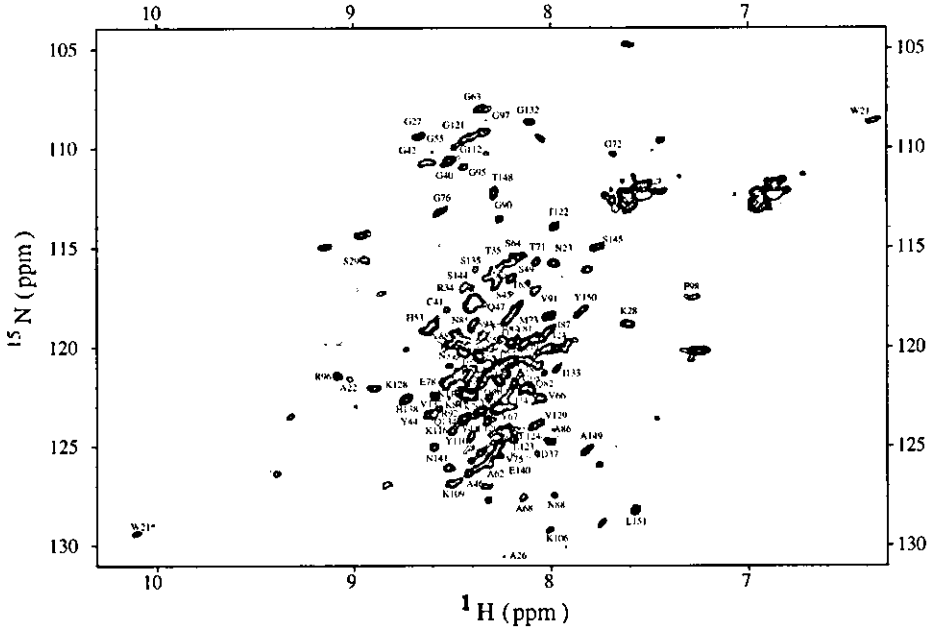

Figure 1. ^{1}H-^{15}N HSQC spectrum of $(His)_6$-LECT2 at 298 K. Amino acid labels were omitted from the middle of the HSQC for clarity. *indicates Trp side chain.

Extent of assignments and data deposition

Most of backbone resonances (90% of ^{15}N, 90% of H^N, 92% of C^α, 76% of H^α, 92% of C^β, and 79% of C′) and a part of aliphatic side-chain resonances have been assigned and deposited in the BioMagResBank (http://www.bmrb.wisc.edu) under an accession number of 6025.

Figure 1 shows the ^{1}H-^{15}N HSQC spectrum of ^{15}N/^{13}C-labeled $(His)_6$-LECT2. A six-residue segment ranging from 100 to 105 and six other residues at positions 19, 24, 25, 38, 51 and 143 remain unassigned as well as the N-terminal His_6-tag. The assignments of these residues have been hampered due to severe overlaps of NMR signals and possible fast exchanges of H^N involved.

The secondary structure prediction by CSI indicates that LECT2 contains several β-strands but no α-helix, which is consistent with the far-UV CD (circular dichroism) data (Ito et al., 2003).

Acknowledgements

This work was supported in part by Grants-in-Aid for Scientific Research and the National Project on Protein Structural and Functional Analyses from the Ministry of Education, Culture, Sports, Science and Technology of Japan.

References

Delaglio, F., Grzesiek, S., Vuister, G.W., Zhu, G., Pfeifer, J. and Bax, A. (1995) *J. Biomol. NMR*, **6**, 277–293.

Hiraki, Y., Inoue, H., Kondo, J., Kamizono, A., Yoshitake, Y., Shukunami, C. and Suzuki, F. (1996) *J. Biol. Chem.*, **271**, 22657–22662.

Ito, M., Nagata, K., Kato, Y. Oda, Y., Yamagoe, S., Suzuki, K. and Tanokura, M. (2003) *Protein Expr. Purif.*, **27**, 272–278.

Kameoka, Y., Yamagoe, S., Hatano, Y., Kasama, T. and Suzuki, K. (2000) *Arthritis Rheumatism*, **43**, 1419–1420.

Shukunami, C., Kondo, J., Wakai, H., Takahashi, K., Inoue, H., Kamizono, A. and Hiraki, Y. (1999) *J. Biochem.*, **125**, 436–442.

Wishart, D.S. and Sykes, B.D. (1994) *J. Biomol. NMR*, **4**, 171–180.

Wishart, D.S., Bigam, C.G., Yao, J., Abildaard, F., Dyson, H.J., Oldfield, E., Markley, J.L. and Sykes, B.D. (1995) *J. Biomol. NMR*, **6**, 135–140.

Yamagoe, S., Mizuno, S. and Suzuki, K. (1998a) *Biochim. Biophys. Acta*, **1396**, 105–113.

Yamagoe, S., Watanabe, T., Mizuno, S. and Suzuki, K. (1998b) *Gene*, **216**, 171–178.

Yamagoe, S., Yamakawa, Y., Matsuo, Y., Minowada, J., Mizuno, S. and Suzuki, K. (1996) *Immunol. Lett.*, **52**, 9–13.

Identification of the Leukocyte Cell-Derived Chemotaxin 2 as a Direct Target Gene of β-Catenin in the Liver

Christine Ovejero,[1] Catherine Cavard,[1] Axel Périanin,[2] Theodorus Hakvoort,[3] Jacqueline Vermeulen,[3] Cécile Godard,[1] Monique Fabre,[4] Philippe Chafey,[1] Kazuo Suzuki,[5] Béatrice Romagnolo,[1] Satoshi Yamagoe,[5] and Christine Perret[1]

To clarify molecular mechanisms underlying liver carcinogenesis induced by aberrant activation of Wnt pathway, we isolated the target genes of β-catenin from mice exhibiting constitutive activated β-catenin in the liver. Adenovirus-mediated expression of oncogenic β-catenin was used to isolate early targets of β-catenin in the liver. Suppression subtractive hybridization was used to identify the leukocyte cell-derived chemotaxin 2 (LECT2) gene as a direct target of β-catenin. Northern blot and immunohistochemical analyses demonstrated that LECT2 expression is specifically induced in different mouse models that express activated β-catenin in the liver. LECT2 expression was not activated in livers in which hepatocyte proliferation was induced by a β-catenin–independent signal. We characterized by mutagenesis the LEF/TCF site, which is crucial for LECT2 activation by β-catenin. We further characterized the chemotactic property of LECT2 for human neutrophils. Finally, we have shown an up-regulation of LECT2 in human liver tumors that expressed aberrant activation of β-catenin signaling; these tumors constituted a subset of hepatocellular carcinomas (HCC) and most of the hepatoblastomas that were studied. In conclusion, our results show that LECT2, which encodes a protein with chemotactic properties for human neutrophils, is a direct target gene of Wnt/β-catenin signaling in the liver. Since HCC develops mainly in patients with chronic hepatitis or cirrhosis induced by viral or inflammatory factors, understanding the role of LECT2 in liver carcinogenesis is of interest and may lead to new therapeutic perspectives. (HEPATOLOGY 2004;40:167–176.)

Hepatocellular carcinoma (HCC), the major primary liver cancer, is becoming increasingly common worldwide.[1] The prognosis for patients with HCC is rather poor. The molecular changes underlying HCC remain largely unknown despite the fact that major risk factors, such as chronic hepatitis B or C infection and exposure to hepatocarcinogens like aflatoxin B1, are well recognized. Several genetic changes have been implicated in at least 3 pathways of carcinogenesis, specifically, the p53, RB and Wnt/β-catenin signaling pathways.[2] Deregulation of the Wnt pathway appears to be most frequent of these changes in human HCC; it occurs in about 30% to 40% of patients.[2,3] It also occurs in more than 90% of hepatoblastomas, which are rare embryonal liver tumors.[4] Mutations affecting 2 partners of the Wnt pathway have been found in liver cancers. One is a mutation that activates the β-catenin gene. Such mutations occur mainly in hepatitis B-negative HCC[5] and in more than 50% of hepatoblastomas.[6,7] The other is a mutation that inactivates the axin 1, and, less commonly, the axin 2 gene.[5,8,9] Mutations that activate the Wnt pathway result in β-catenin accumulation in the nucleus. This process, in association with LEF/TCF transcription factors, modulates the transcription of target genes.[10,11] It is now clear that the genetic program triggered by activation of β-catenin signaling depends on the cellular context. The β-catenin target genes c-myc and cyclin D1 are well

Abbreviations: HCC, hepatocellular carcinoma; GS, glutamine synthetase; LECT2, leukocyte cell-derived chemotaxin 2; SSH, suppression subtractive hybridization; cDNA, complementary DNA; PMN, polymorphonuclear leukocytes; PCR, polymerase chain reaction; HBSS, Hanks' Balanced Salt Solution; ISH, in situ hybridization; SDS-PAGE, sodium dodecyl sulfate-polyacrylamide gel electrophoresis; fMLP, N-formyl-methionyl-leucyl-phenylalanine; RT-PCR, reverse-transcriptase polymerase chain reaction; HA-tagged, influenza hemagglutinin-tagged.

From the [1]Institut Cochin, Département GDPM, Paris, France; [2]Institut Cochin, Département de Biologie Cellulaire, Paris, France; [3]Academic Medical Center, AMC Liver Center, Amsterdam, The Netherlands; [4]Pathology, University school of Medicine of Paris XI and Hospital of Bicêtre Assistance Publique, Paris, France; [5]Department of Bioactive Molecules, National Institute of Infectious Diseases, Shinjuku, Tokyo, Japan.

Received February 18, 2004; accepted March 22, 2004.

Supported by the Comité de Paris de la Ligue Nationale contre le Cancer, the Association pour la Recherche contre le Cancer, and the Ministère Délégué à la Recherche et aux Nouvelles Technologies, ACI Biologie de Développement et Physiologie Intégrative. C.O. is recipient of a fellowship from La Ligue Nationale contre le Cancer.

Address reprint requests to: Dr. Christine Perret, Département de Génétique, Développement et Pathologie Moléculaire, Institut Cochin, 24 rue du Faubourg St Jacques, 75014 Paris, France; E-mail: perret@cochin.inserm.fr; fax: 33 1 44 41 24 21.

Published online in Wiley InterScience (www.interscience.wiley.com).

DOI 10.1002/hep.20286

recognized[12,13]; neither c-myc nor cyclin D1 were induced in the liver of transgenic mice that express an oncogenic form of β-catenin, although such mice exhibit hepatomegaly and marked hepatocellular proliferation.[14] We used several mouse models in which β-catenin signaling in the liver is activated to identify liver-specific target genes of the Wnt pathway that may be implicated in the development of liver cancer. We have identified 3 components of the metabolic pathway of glutamine and have demonstrated that the glutamine synthetase (GS) gene, which is frequently overexpressed in HCC, is a target of β-catenin signaling.[15]

To search for early genes that are sensitive to deregulation of the Wnt/β-catenin pathway in the liver, we used mice infected with an adenovirus that encodes an oncogenic form of β-catenin. We have previously shown that activation of the Wnt pathway using this approach may be achieved as early as 48 hours postinfection.[15] This report describes the identification of a new β-catenin target gene, leukocyte cell-derived chemotaxin 2 (LECT2), which is expressed in the liver.

Materials and Methods

Animals. All procedures involving animals reported in this paper were carried out in accordance with French government regulations (Services Vétérinaires de la Santé et de la Production Animale, Ministère de l'Agriculture). L-PK/c-myc,[3] ΔN131β-catenin,[14] and ASV[16] transgenic mice have been previously described.

Adenoviral Gene Transfer. The adenoviruses AdGFP, AdLacZ, and AdβcatS37A have been described previously.[17] B6D2/F1 mice were injected intravenously with 5×10^9 plaque-forming units of AdGFP, AdLacZ, or AdβcatS37A, and were sacrificed 48 hours later.

Suppression Subtractive Hybridization (SSH). We generated complementary DNA (cDNA) from 1 μg poly(A)+ RNA isolated from the livers of 3 mice injected intravenously with AdβcatS37A (tester) and 6 mice injected intravenously with AdLacZ or AdGFP (driver) using the SMART PCR cDNA Synthesis Kit (BD Biosciences, Paris, France). SSH was undertaken using the PCR-Select cDNA Subtraction Kit (BD Biosciences, Clontech, Palo Alto, CA) according to the manufacturer's protocol. The subtracted cDNA library was subcloned into T/A cloning vector pT-Adv (Clontech, Paris, France) and transformed to ElectroMAX DH10B cells (Invitrogen, Carlsbad, CA). The library was plated on LB-ampicillin plates and incubated at 37°C overnight. Individual clones of the library were plated on LB-ampicillin 96 plates and 2 replicas were made using Hybond N+ (Amersham Biosciences, UK) nylon membranes. For differential screening, replica filters were hybridized with ^{32}P-labeled subtracted tester end driver probes. Blast search was used to analyze sequence homologies in the gene database.

Human Tumor Samples and RNA Sources. All tumor samples were obtained from surgical liver resections. RNA samples were extracted from frozen liver sections. HCC RNA samples were obtained; 29 RNA samples were kindly provided by Dr. Marie-Annick Buendia (Institut Pasteur, France) and 22 RNA samples were extracted from tumor samples obtained at Cochin Hospital (Paris, France). These tumor samples were evaluated for the presence of mutations that activate the β-catenin gene as previously described.[3] Liver specimens were obtained from patients with hepatoblastoma managed at the Bicêtre Hospital (Le Kremlin-Bicêtre, France). All of these patients had received preoperative chemotherapy. Samples were fixed in 10% neutral buffered formalin and were embedded in paraffin. Hepatoblastoma RNA samples were kindly provided by Dr Marie-Annick Buendia (Institut Pasteur, France). According to French law and ethical guidelines, no informed consent is required before analysis of RNA samples from specimens of resected tissue that would otherwise be discarded.

Preparation of Polymorphonuclear Leukocytes. Heparinized human venous blood was obtained from healthy volunteers. Polymorphonuclear leukocytes (PMN) were isolated using a 2-step sedimentation. Whole heparinized (10 units/mL) blood on 2% Dextran T500 in saline was centrifuged, and the granulocyte-rich supernatant was then centrifuged on a Ficoll-Hypaque cushion (Eurobio, Paris, France), as previously described.[18] Purified PMN (95%-97 %) were subjected to hypotonic lysis for 30 seconds, washed, and suspended in Hanks' Balanced Salt Solution (HBSS) containing 1.2 mmol calcium at pH 7.4.

Cell Transfection Studies. Huh7 and HepG2 cells were maintained in DMEM containing 10% (vol/vol) calf serum. Transient transfections were undertaken when cells were 60% to 70% confluent in 12-well plates, using Lipofectamine Plus Reagent (Invitrogen). A TK-Renilla plasmid (10 ng) was included in each transfection as a reference for monitoring transfection efficiency. Cells were lysed 24 hours after transfection and the luciferase and Renilla activities were assayed using Dual Luciferase Reporter Assay (Promega, Madison, WI). All experiments were undertaken in duplicate and were repeated at least 3 times. The total amount of transfected DNA was kept constant by adding the empty expresssion vector pCAN. The ΔN89β-catenin-pCAN expression vector was kindly provided by P. Polakis (San Francisco, CA), and the expression plasmid encoding

ΔNTcf4 was kindly provided by H. Clevers (Utrecht, The Netherlands).

Plasmid Constructs. The sequences of the human and mouse LECT2 genes have already been described.[19,20] The human and mouse promoters were synthesized from human and mouse genomic DNA by polymerase chain reaction (PCR) cloning.[19] *In situ* hybridization (ISH) probes were prepared from full-length human LECT2 cDNA (gi: 4504976) cloned in the *Sma*I site of pSP72 (Promega). Riboprobes were synthesized from linearized *Bgl*II (sense) and *Xho*I (antisense) plasmid. GS riboprobes were generated as previously described.[21]

Northern Blotting. Total RNA was extracted from frozen liver using the guanidium thiocyanate single-step procedure; an aliquot (15 μg) was electrophoresed through 1% agarose-6% formaldehyde gel. The RNA samples were transferred to Hybond N+ (Amersham Pharmacia) membranes and hybridized with the corresponding ^{32}P-labeled probes.

Western Blotting. Tissues were homogenized in Laemmli buffer (1:10 wt/vol). Total proteins (10 μg) were separated using 10% sodium dodecyl sulfate-polyacrylamide gel electrophoresis (SDS-PAGE), and were transferred to a nitrocellulose membrane. LECT2 was detected using polyclonal anti-mouse LECT2.[22] The signals were visualized using the chemiluminescence detection system.

Radioactive* In Situ *Hybridization. The radioactive ISH detection of messenger RNA sequences has been extensively described previously.[21] The LECT2 probes (both orientations) were double-labeled. Slides were exposed for 7 days for GS and 21 days for LECT2.

Chemotactic Assay. *N*-formyl-methionyl-leucyl-phenylalanine (fMLP) was purchased from Sigma (St Louis, MO). Stock solutions were stored in DMSO at −20°C. Recombinant mouse and human LECT2 proteins were produced from CHO cells as previously described.[22] Random and directed migration of PMN was studied using the Boyden chamber technique.[23] Suspensions of 0.5 × 10^6 PMN in 100 μL HBSS containing 1% BSA were incubated in the upper compartment of a chamber separated from the lower compartment by a cellulose filter (3 μm diameter pores; Millipore, Bedford, MA). The lower compartment contained various concentrations of LECT2 or fMLP. In some experiments, the chemoattractant was placed in the PMN chamber to destroy the chemotactic gradient. Chambers were incubated at 37°C for 40 minutes in 95% humidified air; filters were treated with ethanol and stained with hemalum. Unstimulated and directed migrations of PMN were measured as the migration front (at least 10 PMN) under a microscope. Five fields were analyzed for each filter. Results, obtained from 3 experiments, are expressed in micrometers.

Immunohistochemistry. Immunohistochemistry was undertaken using 5 μm sections of formalin-fixed, paraffin-embedded liver. Sections were incubated with specific antibodies for 1 hour. The primary antibodies used were polyclonal anti-mouse LECT2,[20] monoclonal anti-GS (1/200; BD Transduction Laboratories, Lexington, KY), monoclonal anti–β-catenin (1/500; BD Transduction Laboratories) polyclonal anti-GFP (1/50; BD Biosciences), and polyclonal antihemagglutinin (1/400; Clontech: Roche, Basel, Switzerland). LECT2, GS, β-catenin, GFP, and hemagglutinin (HA) were visualized using an immunoperoxidase protocol (Vectastain ABC Kit; Vector, Burlingame, CA). The proliferation marker Ki67 was detected immunohistochemically as previously described.[14]

Real-Time Reverse-Transcriptase (RT)-PCR Analysis. Two μg of total RNA was reverse transcribed in a final volume of 40 μL as previously described.[14]

PCR reactions were undertaken using the LightCycler Instrument (Roche Molecular Biochemicals) and the LightCycler FastStart DNA Master Sybr Green I Reagent Kit (Roche Molecular Biochemicals), according to the manufacturer's protocol. PCR was run in 10 μL total volume (2 μL of diluted cDNA corresponding to 5 ng of total RNA and 8 μL of reaction mix containing 1 μL of 10 μmol of each primer) for 45 cycles. For each tumor sample, 2 reactions, 1 for the target gene and 1 for the reference 18S ribosome RNA, were undertaken in separate capillaries.

Quantification was undertaken using the calibrator-normalized Relative Quantification Software. The relative target gene expression was normalized on the basis of its 18S ribosomal content and to a calibrator which was normal human liver. The calibrator was included in each run and its normalized gene expression was set at a value 1. For each tumoral liver sample, the relative gene expression was expressed as x-fold the realtive expression of the calibrator. Primer sequences were: human LECT2 gene lectF: 5′-GGCAAGTCTTCCAATGA-3′, LectR: 5′CACATGCGATTGTATGC-3′, human GS gene GSF: 5′AAGTGTGTGGAAGAGTTGCC-3′, GSR: 5′-TGC TCACCATGTCCATTATC-3′, 18S gene: 18SF: 5′-GTAACCCGTTGAACCCCATT-3′, 18SR: 5′-CCA TCCAATCGGTAGTAGCG.

Results

Identification of LECT2 Gene by SSH. We used SSH to identify early target genes regulated by Wnt/β-catenin signaling. The livers of mice injected with an ad-

enovirus that encodes for an oncogenic form of β-catenin (AdβcatS37A, HA-tagged) or with control adenoviruses that encode for LacZ or GFP (AdLacZ and AdGFP) were removed 48 hours postinjection and the RNA extracted. The resulting subtracted cDNA library was screened. We isolated four genes that are strongly expressed: the GS gene that we had previously isolated as a hepatic β-catenin target gene,[15] CYP2E1, RNase A family 4, and the LECT2 gene (data not shown). We focused on the LECT2 gene, because our recent results of studies of transgenic mice that lack the LECT2 gene suggested that LECT2 may regulate the homeostasis of natural killer T cells in the liver and may be involved in the pathogenesis of hepatitis LECT2 expression was substantially increased in the livers of mice that had been injected with AdβcatS37A (Fig. 1A). The early expression of LECT2 in response to activated β-catenin was also confirmed in an independent experiment. Livers were obtained from mice that had been sacrificed after injection of AdβcatS37A or control AdGFP. The LECT2 signal began to increase 24 hours after injection and reached a peak at 48 hours; it then remained almost stable for up to 120 hours in AdβcatS37A-infected livers (Fig.1B).

The distribution of LECT2 protein in mouse liver has not been published previously. Immunohistochemical studies showed that LECT2 expression is restricted to the perivenous hepatocytes in normal mouse liver (Fig. 2C). However, LECT2 expression was found throughout the liver lobules of AdβcatS37A-infected mice; the distribution of oncogenic β-catenin, as revealed by HA immunohistochemistry, was similar. Activation of the Wnt pathway was revealed by HA cytosolic and nuclear staining (Fig. 1C). Thus, the targeted activation of the Wnt pathway in hepatocytes induces LECT2 expression in these cells. In contrast, no induction of LECT2 expression was observed in AdGFP-infected livers, even though the livers were infected to about the same extent, as judged by GFP and HA staining (Fig. 1C).

Up-regulation of LECT2 Expression Is Linked to an Activation of β-Catenin Signaling in the Liver. Northern and Western blot analyses demonstrated that LECT2 gene expression is more strongly increased in the liver of ΔN131β-catenin transgenic mice than in the liver of a nontransgenic mouse (wild type; Figs. 2A and B). As expected, LECT2 expression was found throughout the liver lobule where oncogenic β-catenin was present (Fig. 2C).

We also studied L-PK/c-myc mice with liver tumors: more than 50% of the tumors had activating mutations in the β-catenin gene.[3] Our earlier studies of such mice showed that activation of β-catenin signaling in liver tumors was associated with the overexpression of the gene

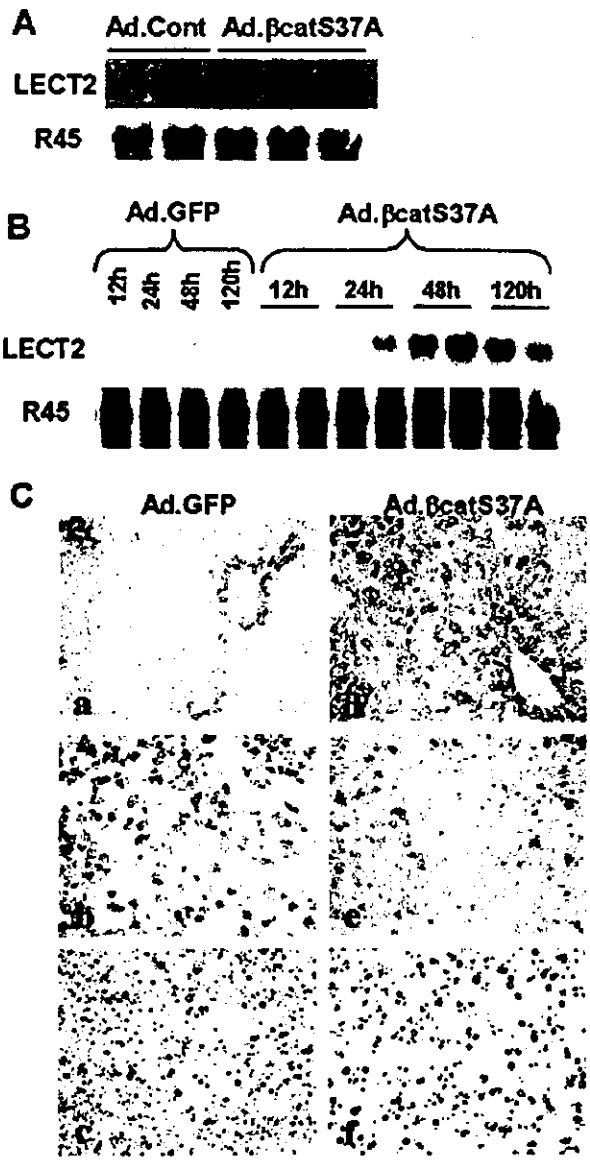

Fig. 1. Identification of LECT2 as a potential β-catenin target gene in infected liver of mice. (A) LECT2 gene expression in adenovirus-infected livers used for the SSH library. RNA samples from livers of mice used for the SSH library, infected with recombinant adenoviruses that encoded for GFP, *Lac Z* (Ad.Cont), or an activated β-catenin (Ad.βcatS37A) were evaluated by Northern blotting. Blots were standardized with ribosomal probe R45. (B) LECT2 gene expression in adenovirus-infected livers. Mice were injected with the indicated adenoviruses and sacrificed 12, 24, 48, or 120 hours after injection (2 mice for each time point). RNA from infected livers was evaluated by Northern blotting. (C) Distribution of LECT2 in adenovirus-infected livers. (a and d) Sections of liver infected with adenoviruses for 120 hours were assessed for distribution of LECT2. (b and e) transgene expression, and (c and f) proliferation by KI-67 immunohistochemical staining. Transgene expression was assessed using (b) GFP immunohistochemical staining and (e) HA immunohistochemical staining that visualized HA-tagged β-catenin S37A. Activation of β-catenin signaling was revealed by cytosolic and nuclear HA immunohistochemical staining. (a, b, and c) Livers infected with adenoviruses encoding GFP (Ad.GFP) for 120 hours. (Magnification, ×200). (d, e, and f) Livers infected by AdβcatS37A for 120 hours.

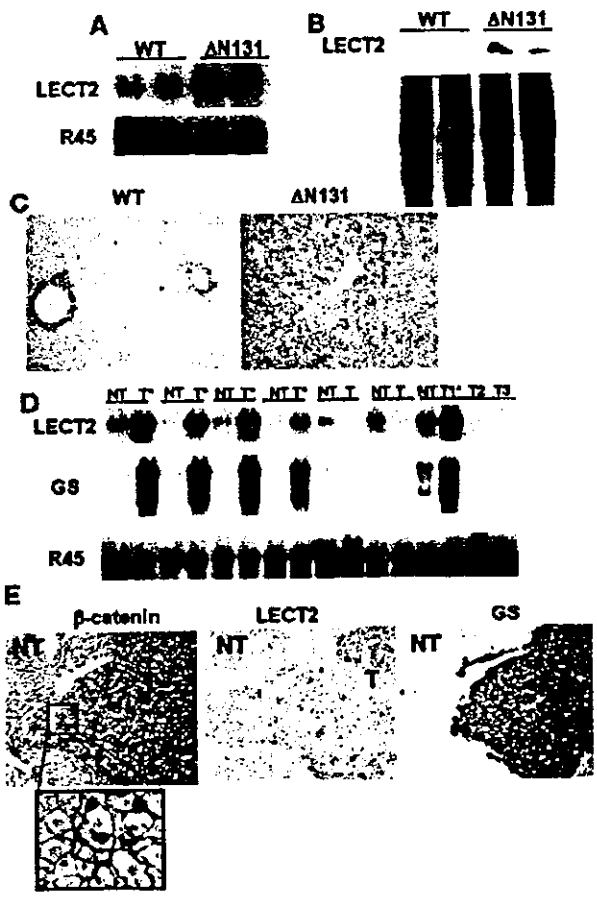

Fig. 2. LECT2 and GS gene expression in the livers of ΔN131β-catenin and PK/c-myc transgenic mice. (A) LECT2 gene expression in ΔN131β-catenin transgenic mice. RNA samples from the liver of wild type (WT) and ΔN131β-catenin transgenic (ΔN131) mice were evaluated by Northern blotting. Blots were standardized using ribosomal probe R45. (B) Western blot analysis of livers from ΔN131β-catenin transgenic mice. Total cell extracts were analyzed using SDS-PAGE and immunoblotted with anti-LECT2 antibody. (C) Sections of the livers of WT and ΔN131β-catenin (ΔN131) mice were stained with an anti-LECT2 antibody. (Magnification, ×200.) (D) Northern blot analysis of RNA from liver tumor tissue (T, T1, T2, T3) from PK/c-myc transgenic mice and nontumor liver (NT). The asterisk (*) marks tumors with activated β-catenin. (E) Immunohistochemical detection of β-catenin, LECT2, and GS in liver tumors from PK/c-myc mice. **(Left)** a representative tumor nodule (T) showing cytosolic and nuclear staining for β-catenin that was not present in nontumor tissue (NT). **(Middle)** Immunohistochemical detection of LECT2 showing uniform staining for LECT2 in the tumor (T). The adjacent nontumoral tissue (NT) exhibits perivenous staining for LECT2. **(Right)** Section with uniform GS staining throughout the tumor (T) and perivenous GS staining in the adjacent nontumor tissue (NT). (Magnification, ×200.) This illustration is representative of 15 liver tumors analyzed.

that encodes for GS.[15] Accordingly, we assayed LECT2 and GS gene expressions in isolated hepatic tumor nodules—with or without activated β-catenin—and compared their expression to that in adjacent nontumor tissue. The expression of LECT2 gene was up-regulated in the tumors associated with activated β-catenin and GS expression. The liver tumors that were negative for GS were also negative for LECT2 (Fig. 2D). Immunohistochemistry revealed that expression of LECT2 was restricted to the perivenous region of nontumor tissue. Both LECT2 and GS were widely distributed throughout tumor tissue in which there was activation of β-catenin signaling, as indicated by positive immunohistochemical staining for β-catenin in the cytosol and, occasionally, in the nucleus (Fig. 2E).

To confirm that the up-regulation of LECT2 expression was associated with activation of β-catenin signaling in the liver, we analyzed the expression of LECT2 in liver tumors that developed in ASV transgenic mice following the expression of SV40 early sequences.[16] The Wnt pathway is not activated in the tumors of such mice[24]. No up-regulation of LECT2 was observed in liver tumors of ASV transgenic mice, although these tumors were highly proliferative (Figs. 3B, C, and D). Absence of induction of LECT2 expression in this model was confirmed by Northern blot analysis (data not shown). We also found no increased LECT2 expression in AdGFP-infected mice, although there was substantial hepatocellular proliferation in this model (Fig. 1C).

LECT2 Is a Downstream Target of the β-Catenin/TCF-4 Signaling Pathway. The identification of several LEF/TCF binding sequences in the mouse and human

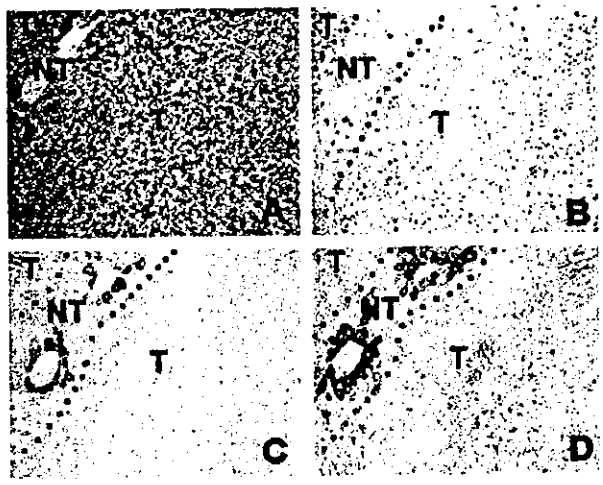

Fig. 3. Distribution of LECT2 and GS in liver tumors from SV40 large T-antigen transgenic mice. Immunohistochemical detection of KI67, LECT2, and GS in liver tumor of SV40 large T-antigen transgenic mice (ASV). (A) Histology, hematoxylin-eosin staining. (B) KI67 staining showing hepatocyte proliferation in tumor tissue (T) and no staining in the adjacent nontumor tissue (NT). (C) Immunohistochemical detection of LECT2. There is perivenous LECT2 staining in the nontumor tissue (NT), no staining for LECT2 in the tumor (T). (D) Immunohistochemical detection of GS. GS staining was similar to that for LECT2: it was restricted to the perivenous region of the nontumoral tissue. (Magnification, ×200.) This illustration is representative of the results obtained from 3 different ASV mice.

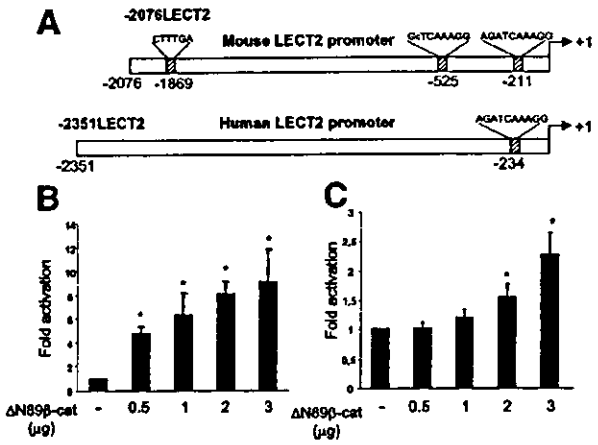

Fig. 4. The mouse and human LECT2 promoters are activated by β-catenin. (A) Diagram showing the mouse LECT2 promoter (−2076LECT2) and the human LECT2 promoter (−2351LECT2). Putative LEF/TCF binding sites are located from the ATG site; the proximal LEF/TCF binding site matched to the consensus LEF/TCF site. It is the same in both the mouse and human LECT2 promoter. (B) Huh7 cells were transfected with 0.1 μg of mouse LECT2 promoter (−2076LECT2-LUC) together with increasing concentrations of activated β-catenin: 0, 0.5, 1, 2, and 3 μg of ΔN89β-catenin-encoding plasmid (ΔN89β-cat). Results are presented as x-fold induction relative to transfection of the reporter by an empty expression vector. The **bars** represent the mean values of 3 experiments, each undertaken in duplicate. **Error bars** represent SEMs. $*P < .05$. (C) Huh7 cells were transfected with 1 μg of human promoter (−2351hLECT2) together with 0, 0.5, 1, 2, and 3 μg of ΔN89β-cat. Results are presented as x-fold induction relative to transfection of the reporter by an empty expression vector. The **bars** represent the mean values of 3 experiments, each undertaken in duplicate. **Error bars** represent SEMs. $*P < .05$.

LECT2 promoters (Fig. 4A) led us to determine whether the LECT2 promoter was a direct transcriptional target for activation by β-catenin. To this end, we used Huh7 and HepG2 hepatoma cell lines which differ in their β-catenin status; Huh7 and HepG2 are wild type and activated mutant, respectively.[3]

The induction of both mouse and human LECT2 promoter activities by β-catenin was demonstrated by transient cotransfection studies in Huh7 cells using promoter-luciferase reporter constructs containing about 2 kbp of 5′-flanking regulatory region of the mouse and human LECT2 genes and an oncogenic ββ-catenin construct (ΔN89β-catenin). The result was a significant dose-dependent increase in the mouse and human promoter activities in response to activated β-catenin. The mouse promoter was activated up to 10-fold (Figs. 4B and C). The effect was strongly inhibited by cotransfection with a dominant-negative TCF-4 expression construct (ΔNTCF4) that prevented transactivation through the LEF/TCF recognition motifs (Fig. 5A). The cotransfection of the ΔNTCF4 expression vector in HepG2 cells, which ex-

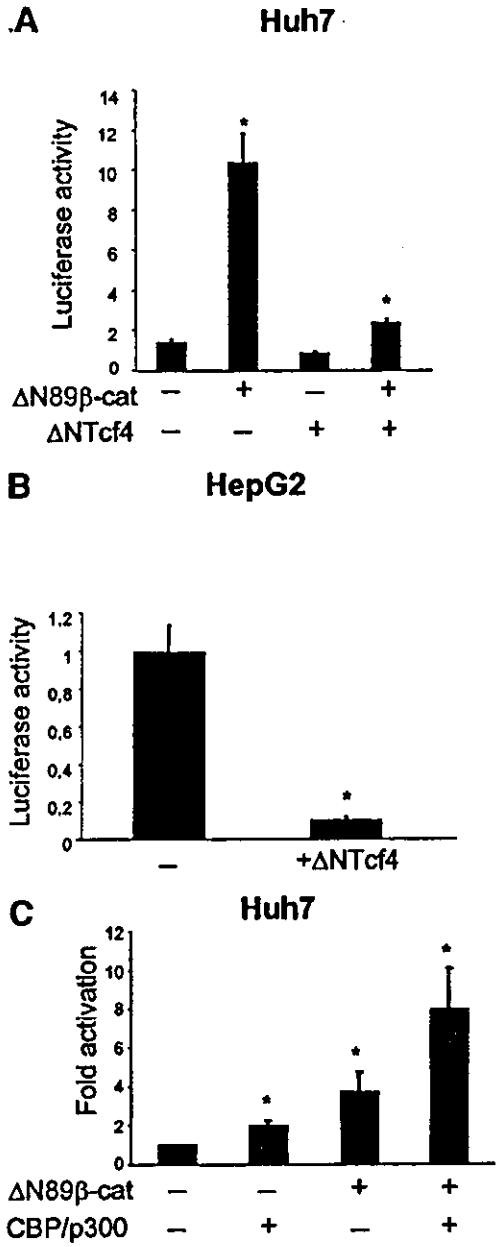

Fig. 5. Control of LECT2 promoter activity by β-catenin: involvement of LEF/TCF sites and the CBP/p300 coactivator. (A)Huh7 cells were transfected with 0.1 μg of mouse LECT2 promoter and 1 μg of β-catenin or empty vector, and 1 μg of ΔNTCF4 expression vector or empty vector. Data are expressed as normalized luciferase activity relative to Renilla control. (B) HepG2 cells were transfected with 0.1 μg of mouse LECT2 promoter and 1 μg of ΔNTCF4 or empty expression vector. Data are expressed as normalized luciferase activity relative to Renilla control. (C) LECT2 promoter transactivation by the CBP/p300 coactivator. Huh7 cells were transfected with 0.1 μg of mouse LECT2 promoter and 0.5 μg of ΔN89β-cat or empty vector, plus 1.5 μg of CBP/p300 or empty vector. Results are presented as x-fold induction relative to transfection of the reporter by empty expression vector. **Bars** represent the means of 3 independent duplicates, each undertaken in duplicates. **Error bars** represent the SD. $*P < .05$.

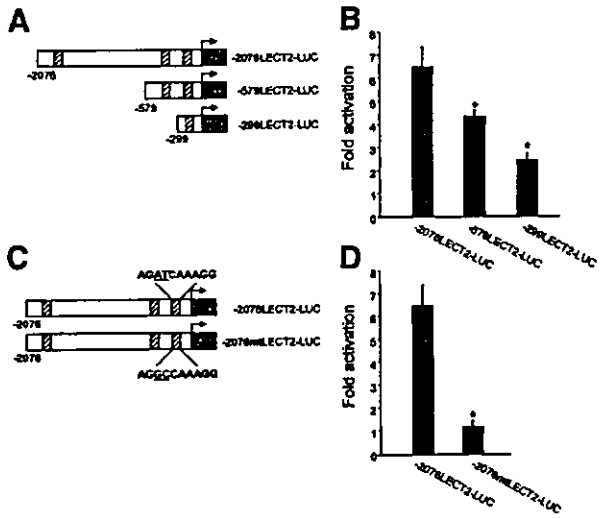

Fig. 6. Role of the proximal LEF/TCF binding sequence of the LECT2 promoter in β-catenin-mediated transactivation (A) Deletion constructs of the mouse LECT2 promoter (−579LECT2-LUC and −299LECT2-LUC) in the pGL3 luciferase reporter plasmid. (B) The deletion constructs of the mouse LECT2 promoter (0.1 μg) were transfected into Huh7 cells as shown in Fig. 5C. (C) The mutated mouse LECT2 reporter construct showing the AT to GC change at nucleotides −209 and −208 (−2076mtLECT2-LUC). D) Huh7 cells were transfected with the wild type or mutated mouse LECT2 reporter construct (0.1 μg) as described in Fig. 5C. Transfections were carried out in triplicate, each undertaken in duplicate. Data are means ± SD. $^*P < .05$.

press an endogenous activated β-catenin, reduced substanially the activity of the LECT2 promoter induced by β-catenin (Fig. 5B). Thus, β-catenin/TCF transactivation controls the activity of the LECT2 promoter. Since the coactivators CBPand p300 have been shown to activate β-catenin/TCF transcription of some Wnt-responsive genes,[25] they could cooperate with β-catenin to activate LECT2 promoter. Transfection with CBP/p300 more than doubled the LECT2 promoter activity induced by β-catenin, whereas the CBP/p300 expression construct alone had little effect on the LECT2 promoter in the absence of β-catenin (Fig. 5C).

Analysis of the mouse promoter shows that it contains 3 potential LEF/TCF binding sequences. To identify the sequences in the LECT2 promoter that can confer transactivation by β-catenin, 2 deletion constructs were generated (Fig. 6A). Analysis of these deletion constructs revealed a progressive decrease of the transactivation induced by β-catenin (Fig. 6B). The smallest construct, which contained only the proximal LEF/TCF site, still mediated a 2- to 3-fold induction of LECT2 promoter activity. This finding indicates that the proximal site could be important in cooperation with distal sites for the transactivation of mouse LECT2 promoter by β-catenin. The proximal LEF/TCF site matched perfectly to the consensus sequence and is conserved in the human LECT2 promoter (Fig. 4A). Thus, this site appears to be a good candidate to support the transcriptional activity of LECT2 promoter by β-catenin. We tested this hypothesis by introducing point mutations in the LEF/TCF proximal site in the full-length LECT2 promoter (−2076mtLECT2-LUC; Fig. 6C). Mutation of the proximal LEF/TCF binding site completely abolished transactivation of the LECT2 promoter by β-catenin (Fig. 6D).

LECT2 is therefore a direct transcriptional target of β-catenin.

Chemotactic Properties of LECT2. The LECT2 protein was initially purified from the culture fluid of phytohemagglutinin-activated human T-cell leukemia SKW-3 cells as a possible chemotactic factor for human neutrophils.[26]

To further characterize the chemotactic property of LECT2, we used a recombinant LECT2 protein produced from CHO cells[22] and tested its chemotactic properties using human PMN. The chemotactic activity of LECT2 was compared to that of the tripeptide fMLP, which is a potent neutrophil chemoattractant.[18,27] LECT2 induced a bell-shaped migration pattern as a function of its concentration; this finding is characteristic of a chemotactic ligand (Fig. 7). Significant directed migration was observed in the presence of 10 to 25 nM LECT2, whereas at a high concentration (50 nmol) LECT2 was inactive, presumably because of chemotactic desensitization of PMN. fMLP induced more directed migration over a wider active concentration range than LECT2. To determine whether the stimulated migration induced by LECT2 may be mediated by chemokinetic activity of PMN, we abolished the chemotactic gradient by titrating LECT2 or fMLP into the cell compartment of the Boyden chamber. Under these conditions, the directed PMN migration was completely prevented (data not shown). This finding confirms that LECT2 is a chemoattractant for human neutrophils.

Expression of the LECT2 Gene in Human Liver Tumors. To investigate if LECT2 could be implicated in human liver cancer, we analyzed LECT2 gene expression using real-time RT-PCR of liver tumors in which the Wnt pathway is frequently altered. We first quantified the relative degree of RNA expression of LECT2 and GS in 18 human HCC samples, in which there were activated mutations of the β-catenin gene. As expected, all these tumors exhibited a high degree of GS expression.[15] In contrast, LECT2 expression was up-regulated in only 5 of these tumors (Fig. 8). Analysis of 33 HCC samples that did not display β-catenin mutations indicated up-regulation of LECT2 in only 6 samples. Interestingly, all of the

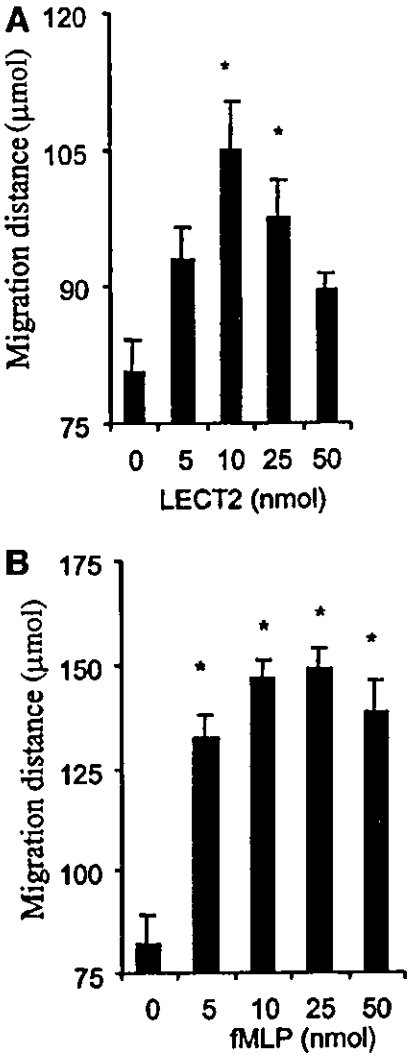

Fig. 7. PMN chemotactic activity of LECT2 and fMLP. The migration of PMN was measured in the presence or absence of various concentrations of (A) LECT2 or (B) fMLP placed in the lower compartment of the Boyden chamber. Results represent the migration front expressed in micrometers (mean ± SEM of 5 individual fields for each concentration, from a representative experiment). The significance of differences between data obtained from 3 independent experiments with random and stimulated migrations were determined using Student's *t* test. $^*P < .05$.

6 LECT2-positive HCC samples were also positive for GS, suggesting that these samples may have mutations of another partner of the Wnt pathway (Fig. 8). Altogether, these results indicated that even though LECT2 was generally down-regulated in human HCC samples, LECT2 was up-regulated only in a subset of human HCC, a subset in which the Wnt pathway was altered. We also analyzed hepatoblastoma samples; deregulation of the Wnt pathway occurs in more than 90% of these tumors[4] We analyszed LECT2 expression in 14 samples using real-time RT-PCR. A high level of LECT2 expression was observed in 13 samples. Overexpression of GS was substantial in all of the samples tested (Fig. 8). ISH, used to localize LECT2 expression, confirmed that LECT2 was up-regulated in hepatoblastomas. LECT2 was detected in the tumor areas that exhibited activation of β-catenin signaling associated with GS expression (Fig. 9).

Discussion

The Wnt pathway is frequently deregulated in carcinogenesis. Considerable effort is currently being made to identify the downstream β-catenin target genes; those that have been identified may be important for understanding the role of Wnt signaling in carcinogenesis because they are involved in cell proliferation, survival, differentiation, and migration.[10,11] However, it has become clear that the Wnt response is tissue-specific. Ex-

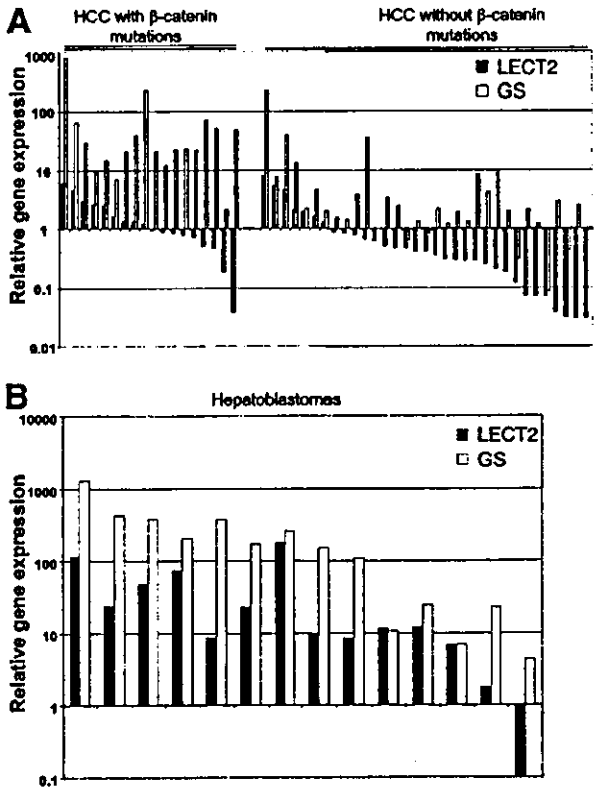

Fig. 8. Up-regulation of LECT2 in human liver tumors Histograms on a logarithmic scale showing the relative expression of LECT2 and GS genes measured in (A) a panel of hepatocellular carcinomas (HCC) with β-catenin mutations and a panel of HCC that have no activating mutations of β-catenin, and (B) in a panel of hepatoblastomas. Relative gene expression was determined using real-time RT-PCR, as described in Materials and Methods, and was expressed as fold difference relative to normal liver, after normalization of each measurement to 18S ribosomal RNA.

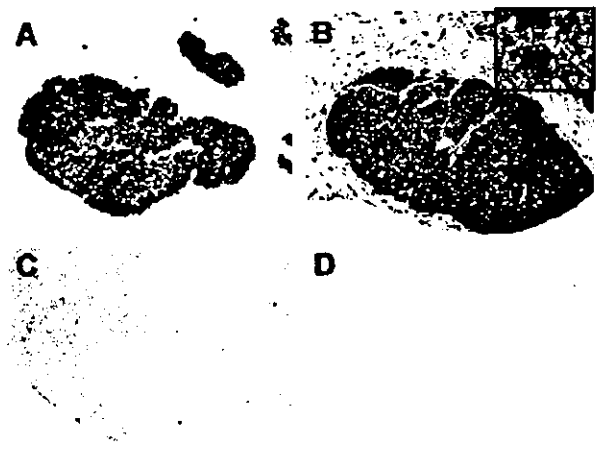

Fig. 9. Expression of LECT2, GS, and β-catenin in hepatoblastoma by *in situ* hybridization. Representative *in situ* hybridization of [^{35}S]-labeled probes for (A) GS antisense, (C) LECT2 antisense, and (D)LECT2 sense in serial sections of a single hepatoblastoma. This illustration is representative of 11 cases analyzed. (Magnification, ×40.) (B) Immunohistochemical staining of β-catenin. Note the tumor area displayed activated β-catenin signaling, as revealed by cytosolic and nuclear accumulation of β-catenin, that parallels the signals of LECT2 and GS. (Magnification, ×40.) (**Insert**) β-catenin cytosolic and nuclear accumulation. (Magnification, ×400.)

pression of activated β-catenin is sufficient to induce polyposis in the intestine[28,29] but is not sufficient to induce hepatocarcinogenesis in the liver. We and others have observed substantial hepatomegaly in response to activation of β-catenin signaling in the liver, but other genetic events are likely to be required for hepatic tumorigenesis.[14,30] Therefore, it is important to identify the target genes of β-catenin in the liver. We used an adenovirus-mediated expression of activated β-catenin to isolate early target genes. We identified the LECT2 gene as a direct target of β-catenin signaling in the liver.

We found that LECT2 promoter activity is increased considerably by activation of β-catenin, and is blocked by a dominant-negative form of TCF-4. We have also identified the LEF/TCF site as being crucial for a response to β-catenin. Our studies in mice with activated β-catenin showed that β-catenin signaling strongly induced LECT2 expression in hepatocytes. As LECT2 is mainly expressed in the liver, we assessed whether LECT2 could be a liver-specific response of the Wnt pathway. We analyzed LECT2 expression in another tumor in which activation of the Wnt pathway is frequent: colon cancer. We observed no induction of LECT2 expression in intestinal epithelial cells of polyps that develop in a mouse model of colon cancer that we recently developed (Colnot et al., unpublished manuscript). Such mice have a new germline mutation of the *Apc* gene and a high level of activation of β-catenin signaling, as indicated by cytosolic and nuclear staining of β-catenin in all epithelial cells of their polyps. So far, few β-catenin target genes have been isolated from liver.[15,31] LECT2 can be induced by β-catenin in the liver but not in the intestine, and it may be an important target relating to the tissue-specific response of the Wnt pathway in hepatic tissue.

Interestingly, LECT2 gene expression is confined to a well-defined pericentral compartment, consisting of 1 to 2 layers of hepatocytes in the normal mouse liver; this expression is similar to that of 3 other hepatic β-catenin-induced genes linked to glutamine metabolism that we identified previously.[15] The zonation of the liver lobule is determined during development of the liver; the molecular mechanisms involved are not known. From our results, it is tempting to speculate that the Wnt pathway in the liver may participate in the establishment of zonation.

The relevance of LECT2 in human liver carcinogenesis has been addressed by examining the level of expression of LECT2 in human liver tumors. We found substantial induction of LECT2 in most of the hepatoblastomas studied; in this tumor, activation of the Wnt pathway is frequent.[4] In contrast, an up-regulation of LECT2 was found only in a subset of HCCs associated with activation of the Wnt pathway. However, LECT2 expression was generally decreased in human HCCs in accordance with previously published findings.[32,33] Hepatoblastoma and HCC are 2 primary liver tumors that differ with respect to their histological manifestations and genetic changes. HCC is a heterogeneous tumor associated with multiple genetic changes; only a limited number of chromosomal changes have been found in hepatoblastomas.[4] The loss of LECT2 expression in HCCs that have aberrant β-catenin signaling could result from "cross-talking" with one or more other signaling pathways induced by different genetic changes that may occurr during tumor progression. At present, the role of LECT2 in liver carcinogenesis is unknown. LECT2 was first isolated as a possible chemotactic factor for neutrophils.[26] Using recombinant protein, we have further characterized the chemotactic property of LECT2 for human neutrophils *in vitro*. We searched for leukocyte infiltration in tumors that overexpressed LECT2, such as those associated with L-PK/c-myc, but we did not find any evidence of an inflammatory process in such tumors. Two hypotheses may be proposed: (1) leukocyte infiltration may be a transient event that cannot be observed in the tumor, and (2) the role of LECT2 in liver carcinogenesis may be linked to another function of LECT2. The study of transgenic mice lacking the LECT2 gene revealed that the role of LECT2 is related to the homeostasis of NKT cells in the liver; LECT2 may modulate the inflammatory and immune response

induced by the development of the tumor. Since HCC develops most commonly in patients with chronic hepatitis or cirrhosis induced by viral or inflammatory factors, understanding the role of LECT2 in liver carcinogenesis is of interest and may lead to new therapeutic perspectives.

Acknowledgment: We thank Professor Axel Kahn for strong support and for critically reading the manuscript, and all the members of our team for helpful discussion. We also thank M. A. Buendia (Institut Pasteur, France) for providing HCC and hepatoblastoma RNA samples, Professor Benoit Terris (Hôpital Cochin, Service d'Anatomopathologie) for providing frozen HCC samples, J. Kitajewski (Columbia University, NY) for providing the recombinant adenoviruses, F. Letourneur and N. Lebrun (Institut Cochin) for sequencing, and Dr. Owen Parkes for editing the manuscript.

References

1. Bosch FX, Ribes J, Borras J. Epidemiology of primary liver cancer. Semin Liver Dis 1999;19:271–285.
2. Buendia MA. Genetics of hepatocellular carcinoma. Semin Cancer Biol 2000;10:185–200.
3. de La Coste A, Romagnolo B, Billuart P, Renard CA, Buendia MA, Soubrane O, et al. Somatic mutations of the beta-catenin gene are frequent in mouse and human hepatocellular carcinomas. Proc Natl Acad Sci USA 1998;95:8847–8851.
4. Buendia MA. Genetic alterations in hepatoblastoma and hepatocellular carcinoma: common and distinctive aspects. Med Pediatr Oncol 2002;39: 530–535.
5. Laurent-Puig P, Legoix P, Bluteau O, Belghiti J, Franco D, Binot F, et al. Genetic alterations associated with hepatocellular carcinomas define distinct pathways of hepatocarcinogenesis. Gastroenterology 2001;120:1763–1773.
6. Wei Y, Fabre M, Branchereau S, Gauthier F, Perilongo G, Buendia MA. Activation of beta-catenin in epithelial and mesenchymal hepatoblastomas. Oncogene 2000;19:498–504.
7. Koch A, Denkhaus D, Albrecht S, Leuschner I, von Schweinitz D, Pietsch T. Childhood hepatoblastomas frequently carry a mutated degradation. Cancer Res 1999;59:269–273.
8. Satoh S, Daigo Y, Furukawa Y, Kato T, Miwa N, Nishiwaki T, et al. AXIN1 mutations in hepatocellular carcinomas, and growth suppression in cancer cells by virus-mediated transfer of AXIN1. Nat Genet 2000;24: 245–250.
9. Taniguchi K, Roberts LR, Aderca IN, Dong X, Qian C, Murphy LM, et al. Mutational spectrum of beta-catenin, AXIN1, and AXIN2 in hepatocellular carcinomas and hepatoblastomas. Oncogene 2002;21:4863–4871.
10. Polakis P. Wnt signaling and cancer. Genes Dev 2000;14:1837–1851.
11. Giles RH, van Es JH, Clevers H. Caught up in a Wnt storm: Wnt signaling in cancer. Biochim Biophys Acta 2003;1653:1–24.
12. He TC, Sparks AB, Rago C, Hermeking H, Zawel L, da Costa LT, et al. Identification of c-MYC as a target of the APC pathway. Science 1998; 281:1509–1512.
13. Tetsu O, McCormick F. Beta-catenin regulates expression of cyclin D1 in colon carcinoma cells. Nature 1999;398:422–426.
14. Cadoret A, Ovejero C, Saadi-Kheddouci S, Souil E, Fabre M, Romagnolo B, et al. Hepatomegaly in transgenic mice expressing an oncogenic form of beta- catenin. Cancer Res 2001;61:3245–3249.
15. Cadoret A, Ovejero C, Terris B, Souil E, Levy L, Lamers WH, et al. New targets of beta-catenin signaling in the liver are involved in the glutamine metabolism. Oncogene 2002;21:8293–8301.
16. Bennoun M, Grimber G, Couton D, Seye A, Molina T, Briand P, et al. The amino-terminal region of SV40 large T antigen is sufficient to induce hepatic tumours in mice. Oncogene 1998;17:1253–1259.
17. Young CS, Kitamura M, Hardy S, Kitajewski J. Wnt-1 induces growth, cytosolic beta-catenin, and Tcf/Lef transcriptional activation in Rat-1 fibroblasts. Mol Cell Biol 1998;18:2474–2485.
18. Perianin A, Pedruzzi E, Hakim J. W-7, a calmodulin antagonist, primes the stimulation of human neutrophil respiratory burst by formyl peptides and platelet-activating factor. FEBS Lett 1994;342:135–138.
19. Yamagoe S, Kameoka Y, Hashimoto K, Mizuno S, Suzuki K. Molecular cloning, structural characterization, and chromosomal mapping of the human LECT2 gene. Genomics 1998;48:324–329.
20. Yamagoe S, Mizuno S, Suzuki K. Molecular cloning of human and bovine LECT2 having a neutrophil chemotactic activity and its specific expression in the liver. Biochim Biophys Acta 1998;1396:105–113.
21. Moorman AF, Houweling AC, de Boer PA, Christoffels VM. Sensitive nonradioactive detection of mRNA in tissue sections: novel application of the whole-mount in situ hybridization protocol. J Histochem Cytochem 2001;49:1–8.
22. Yamagoe S, Akasaka T, Uchida T, Hachiya T, Okabe T, Yamakawa Y, et al. Expression of a neutrophil chemotactic protein LECT2 in human hepatocytes revealed by immunochemical studies using polyclonal and monoclonal antibodies to a recombinant LECT2. Biochem Biophys Res Commun 1997;237:116–120.
23. Boyden S. The chemotactic effect of mixture of antibody and antigen on polymorphonuclear leukocytes. J Exp Med 1962;115:453–466.
24. Umeda T, Yamamoto T, Kajino K, Hino O. beta-catenin mutations are absent in hepatocellular carcinomas of SV40 T-antigen transgenic mice. Int J Oncol 2000;16:1133–1136.
25. Hecht A, Vleminckx K, Stemmler MP, van Roy F, Kemler R. The p300/CBP acetyltransferases function as transcriptional coactivators of beta-catenin in vertebrates. EMBO J 2000;19:1839–1850.
26. Yamagoe S, Yamakawa Y, Matsuo Y, Minowada J, Mizuno S, Suzuki K. Purification and primary amino acid sequence of a novel neutrophil chemotactic factor LECT2. Immunol Lett 1996;52:9–13.
27. Chenoweth DE, Rowe JG, Hugli TE. A modified method for chemotaxis under agarose. J Immunol Methods 1979;25:337–353.
28. Romagnolo B, Berrebi D, Saadi-Keddoucci S, Porteu A, Pichard AL, Peuchmaur M, et al. Intestinal dysplasia and adenoma in transgenic mice after overexpression of an activated beta-catenin. Cancer Res 1999;59:3875–3879.
29. Harada N, Tamai Y, Ishikawa T, Sauer B, Takaku K, Oshima M, et al. Intestinal polyposis in mice with a dominant stable mutation of the beta-catenin gene. EMBO J 1999;18:5931–5942.
30. Harada N, Miyoshi H, Murai N, Oshima H, Tamai Y, Oshima M, et al. Lack of tumorigenesis in the mouse liver after adenovirus-mediated expression of a dominant stable mutant of beta-catenin. Cancer Res 2002;62: 1971–1977.
31. Levy L, Neuveut C, Renard CA, Charneau P, Branchereau S, Gauthier F, et al. Transcriptional activation of interleukin-8 by beta-catenin-Tcf4. J Biol Chem 2002;277:42386–42393.
32. Uchida T, Nagai H, Gotoh K, Kanagawa H, Kouyama H, Kawanishi T, et al. Expression pattern of a newly recognized protein, LECT2, in hepatocellular carcinoma and its premalignant lesion. Pathol Int 1999;49:147–151.
33. Okabe H, Satoh S, Kato T, Kitahara O, Yanagawa R, Yamaoka Y, et al. Genome-wide analysis of gene expression in human hepatocellular carcinomas using cDNA microarray: identification of genes involved in viral carcinogenesis and tumor progression. Cancer Res 2001;61:2129–2137.

Increase in Hepatic NKT Cells in Leukocyte Cell-Derived Chemotaxin 2-Deficient Mice Contributes to Severe Concanavalin A-Induced Hepatitis[1]

Takeshi Saito,* Akinori Okumura,* Hisami Watanabe,† Masahide Asano,[2‡] Akiko Ishida-Okawara,* Junko Sakagami,‡ Katsuko Sudo,‡ Yoshimi Hatano-Yokoe,§ Jelena S. Bezbradica,¶ Sebastian Joyce,¶ Toru Abo,‖ Yoichiro Iwakura,‡ Kazuo Suzuki,* and Satoshi Yamagoe[3]*

Leukocyte cell-derived chemotaxin 2 (LECT2) was originally identified for its possible chemotactic activity against human neutrophils in vitro. It is a 16-kDa protein that is preferentially expressed in the liver. Its homologues have been widely identified in many vertebrates. Current evidence suggests that LECT2 may be a multifunctional protein like cytokines. However, the function of LECT2 in vivo remains unclear. To elucidate the role of this protein in vivo, we have generated LECT2-deficient ($LECT2^{-/-}$) mice. We found that the proportion of NKT cells in the liver increased significantly in $LECT2^{-/-}$ mice, although those of conventional T cells, NK cells, and other cell types were comparable with those in wild-type mice. Consistent with increased hepatic NKT cell number, the production of IL-4 and IFN-γ was augmented in $LECT2^{-/-}$ mice upon stimulation with α-galactosylceramide, which specifically activates Vα14 NKT cells. In addition, NKT cell-mediated cytotoxic activity against syngeneic thymocytes increased in hepatic mononuclear cells obtained from $LECT2^{-/-}$ mice in vitro. Interestingly, the hepatic injury was exacerbated in $LECT2^{-/-}$ mice upon treatment with Con A, possibly because of the significantly higher expression of IL-4 and Fas ligand. These results suggest that LECT2 might regulate the homeostasis of NKT cells in the liver and might be involved in the pathogenesis of hepatitis. *The Journal of Immunology*, **2004, 173: 579–585.**

Leukocyte cell-derived chemotaxin 2 (LECT2)[4] was originally identified from the culture fluid of the human T cell line SKW-3 in the process of screening for a novel neutrophil chemotactic protein (1). LECT2 is expressed preferentially in the liver in a constitutive manner. LECT2 protein is secreted into the bloodstream (2, 3). Proteins homologous to LECT2 have been isolated in many vertebrates (4, 5). LECT2 is identical with chondromodulin II, which was identified as a growth stimulator for chondrocytes and osteoblasts (6). The polymorphism of human LECT2 at $Val^{58}Ile$ is associated with the severity of rheumatoid arthritis in the Japanese population (7). We recently reported that the expression of mouse LECT2 was transiently decreased during Con A-induced hepatitis, an experimental model for human autoimmune hepatitis that is induced by the expression of cytokines and cytotoxic molecules associated with effects from other immune cells, such as $CD4^+$ T lymphocytes and macrophages (8). Thus, LECT2 seems to be a multifunctional protein like cytokines. However, the function of LECT2 in vivo remains unclear.

NKT cells form a distinctive T cell subpopulation that has some of the characteristics of NK cells. NKT cells are present in various lymphoid organs and are especially abundant in the liver (9–11). In mice, NKT cells commonly express a semi-invariant TCR and NK1.1 Ag, and their development and functions are regulated by CD1d (9, 12). There is growing evidence that NKT cells play an important role in immune responses (9–13). It is well established that NKT cells express large amounts of cytokines, especially IFN-γ and IL-4, and their functional disorders are characteristic of various diseases (9, 12, 13). Recently, some groups reported that NKT cells played an essential role in Con A-induced hepatitis (14–16).

In this study we generated $LECT2^{-/-}$ mice with the aim of clearly identifying the role of LECT2 in vivo. We found that these mice showed an increased number of hepatic NKT cells, which appeared to function as they do in wild-type mice. To examine the biological effect of this phenotype, we used a Con A-induced hepatitis model. The deficiency of LECT2 led to severe liver injury, possibly because of excessive expression of IL-4 and Fas ligand (FasL) by the increase in the number of hepatic NKT cells.

Materials and Methods

Mice

Wild-type C57BL/6J (B6) mice purchased from CLEA Japan were housed at the National Institute of Infectious Diseases. Mice used in this study

*Department of Bioactive Molecules, National Institute of Infectious Diseases, Tokyo, Japan; †Division of Cellular and Molecular Immunology, Center of Molecular Biosciences, University of Ryukyus, Okinawa, Japan; ‡Center for Experimental Medicine, Institute of Medical Science, University of Tokyo, Tokyo, Japan; §Department of Internal Medicine, Showa University, Tokyo, Japan; ¶Department of Microbiology and Immunology, Vanderbilt University School of Medicine, Nashville, TN 37232; and ‖Department of Immunology, Niigata University School of Medicine, Niigata, Japan

Received for publication October 16, 2003. Accepted for publication April 28, 2004.

The costs of publication of this article were defrayed in part by the payment of page charges. This article must therefore be hereby marked *advertisement* in accordance with 18 U.S.C. Section 1734 solely to indicate this fact.

[1] This work was supported by grants from the Japan Health Sciences Foundation; the Ministry of Health, Labor, and Welfare of Japan; the Ministry of Education, Culture, Sports, Science, and Technology of Japan; and National Institutes of Health Grant AI42284.

[2] Current address: Division of Transgenic Animal Science, Advanced Science Research Center, Kanazawa University, Kanazawa 920-8640, Japan.

[3] Address correspondence and reprint requests to Dr. Satoshi Yamagoe, Department of Bioactive Molecules, National Institute of Infectious Diseases, 1-23-1 Toyama, Shinjuku-ku, Tokyo 162-8640, Japan. E-mail address: syamagoe@nih.go.jp

[4] Abbreviations used in this paper: LECT2, leukocyte cell-derived chemotaxin 2; FasL, Fas ligand; α-GalCer, α-galactosylceramide; GPT, glutamic pyruvic transaminase; MNC, mononuclear cell.

0022-1767/04/$02.00

were maintained under specific pathogen-free conditions and were usually used at 8–12 wk of age according to the guidelines of the National Institute of Infectious Diseases animal care and use committee.

Generation of LECT2$^{-/-}$ mice

To construct the targeting vector (pKO-9), two fragments (5′ end, 7.7 kb; 3′ end, 1.4 kb) of the genomic DNA flanking the coding region of the 129-derived *lect2* gene (17) were subcloned between the *Bam*HI and *Spe*I sites and between the *Aat*I and *Sca*I sites of the pBluescript II KS$^+$ vector (Stratagene, La Jolla, CA), respectively. The pGKneobpA cassette (18) was inserted between *Spe*I and *Aat*I for positive selection (Fig. 1*A*). The DT-A cassette (19) was ligated at the 5′ end of the targeting vector for negative selection. E14.1 ES cells (1×10^7 cells) were transferred with the linearized targeting vector by electroporation and were selected with G418 (Invitrogen, Carlsbad, CA). Homologous recombinants were screened by PCR and confirmed by Southern blot hybridization (Fig. 1*A*; data not shown). The forward primer (P2) in the pGKneobpA cassette was 5′-GGTGGATGTG GAATGTGTGC-3′, and the reverse primer (P5) outside the targeting vector was 5′-ACCATCTACTAGCTCTTGTAG-3′. Chimeric mice were generated by the aggregation method (19) with some modifications. The chimeras were mated with B6 mice, and homozygous mutant mice were generated by the intercrossing of heterozygotes. LECT2$^{-/-}$ mice and littermates were genotyped by PCR (Fig. 1*B*). The primer sequences used were as follows: LECT2-common, 5′-CCACCCCACCTAAGATGTATGCTGC-3′; LECT2-wild-type, 5′-CCAGGATTCTAATGTCGTCCTTGTTGG-3′; and LECT2-knockout, 5′-CCTTCTTGACGAGTTCTTCTGAGGGG-3′.

Immunoblot analysis

Two micrograms of serum prepared from LECT2$^{-/-}$ mice and their littermates was resolved by SDS-PAGE (4–20%) and transferred to Immobilon-P (Millipore, Bedford, MA). The blots were incubated with rabbit anti-mouse LECT2 against a recombinant mouse LECT2 produced stably by CHO cells. The immunoreactive protein was visualized using an ECL kit (Amersham Pharmacia Biotech, Piscataway, NJ).

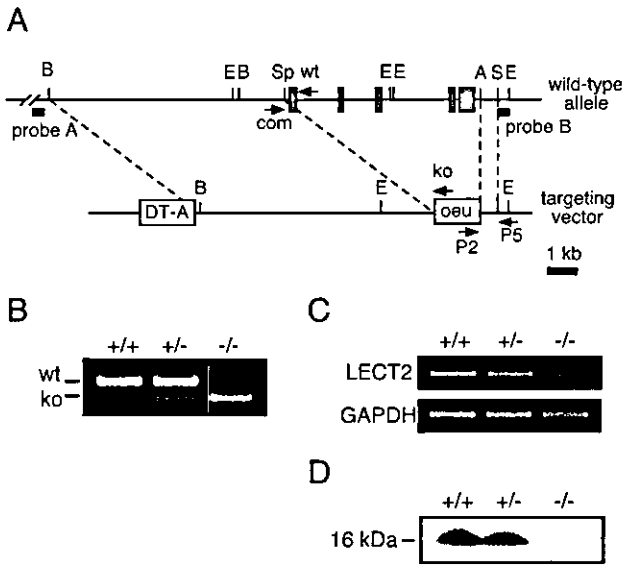

FIGURE 1. Generation of LECT2$^{-/-}$ mice. *A*, Endogenous *Lect2* gene and targeting vector. A 6.4-kb *Spe*I-*Aat*I fragment containing all exons for LECT2 was replaced with pGKneobpA. A, *Aat*I; B, *Bam*HI; E, *Eco*RI; S, *Sca*I; Sp, *Spe*I. Arrows indicate primers for genotyping. Probes A and B were used to confirm the correct recombination by Southern blot analysis. PCR primer LECT2-common (com), LECT2-wild type (wt), and LECT2-knockout (ko) were used for genotyping. *B*, Genotyping of LECT2$^{-/-}$ mice and littermates. Genomic DNA from embryonic stem cells or mouse tails were analyzed by PCR. This analysis yields 517- and 385-bp bands for the wild-type and targeted alleles, respectively. *C*, Total liver RNAs were reverse transcribed and subjected to PCR analysis. The primers used are described in *Materials and Methods*. *D*, Serum from mice was analyzed by Western blot analysis using rabbit anti-LECT2 polyclonal Ab (2).

Lymphocyte preparations

Mice anesthetized with ether were killed by exsanguination via the axillary artery. The liver and spleen were then removed. Hepatic mononuclear cells (MNCs) were prepared as described previously (20). Briefly, the liver lobes were minced to small pieces, pressed through 200-gauge stainless steel mesh, and suspended in Eagle's MEM (Sigma-Aldrich, St. Louis, MO) supplemented with 5 mM HEPES (pH 7.5) and 2% FBS. After washing, the pellet was resuspended in 35% Percoll solution (Amersham Pharmacia Biotech) containing heparin (100 U/ml) and centrifuged at 2000 rpm for 15 min. The pellet was then resuspended in RBC lysis solution (155 mM NH_4Cl, 10 mM $KHCO_3$, 1 mM EDTA, and 17 mM Tris, pH 7.3) and washed twice with MEM. Splenocytes were prepared by forcing minced spleens through stainless steel mesh and were used after RBC lysis.

Flow cytometric analysis

Single-cell suspensions from the liver and spleen were incubated with mAbs against cell surface markers (BD Pharmingen, San Diego, CA). PE-labeled CD1d-α-galactosylceramide (CD1d-α-GalCer) tetramer (21) and FITC-, PE-, allophycocyanin-, or PerCP-conjugated Abs specific for murine CD3 (145-2C11), CD4 (RM4-5), NK1.1 (PK136), Gr-1 (RB6-8C5), Mac-1 (M1/70), and FasL (MFL-3) were used for flow cytometric analyses. Apoptotic cells were stained with an Annexin V-FITC Apoptosis Detection I kit (BD Pharmingen) and then analyzed with FACSCalibur using CellQuest software (BD Biosciences, San Jose, CA).

Administration of α-GalCer

α-GalCer was kindly provided by Kirin Brewery (Gunma, Japan). This reagent was dissolved in 0.5% polysorbate 20 (Nikko Chemical, Tokyo, Japan) at a concentration of 200 μg/ml, then further diluted with physiological saline. For in vivo administration, α-GalCer was injected i.p. at a dose of 100 μg/kg body weight. For in vitro stimulation of MNCs, α-GalCer was added to the culture medium (RPMI 1640 supplemented with 2% FBS) at a concentration of 100 ng/ml.

Cytotoxicity assays

The cytotoxicity assays were performed by a method previously described (22). Briefly, YAC-1 cells and B6 thymocytes for target cells were labeled with sodium [^{51}Cr]chromate (Amersham Pharmacia Biotech) for 2 h and washed three times with RPMI 1640. Effector cells were serially diluted and mixed with ^{51}Cr-labeled target cells ($1–2 \times 10^4$ cells) in a U-bottom, 96-well microculture plate. The plates were centrifuged and incubated for 4 h at 37°C. At the end of the culture, 100 μl of the supernatant was determined by adding RPMI 1640. Maximum release was determined by adding 1 M HCl. The percentage of specific release was calculated as [(experimental release − spontaneous release)/(maximum release − spontaneous release)] × 100.

Con A-induced liver injury

Male B6 (wild-type controls) and LECT2$^{-/-}$ B6 mice were injected i.v. with 25 mg/kg Con A (type IV; Sigma-Aldrich). Two, 5, and 8 h after Con A injection, sera were collected to measure the level of cytokines and glutamic pyruvic transaminase (GPT) activity, and liver tissue was removed to detect the cytokine mRNAs and for immunohistochemical analysis.

Cytokine and transaminase measurement

The levels of serum IFN-γ, TNF-α, and IL-4 were quantified using an OptEIA ELISA set (BD Pharmingen). Serum GPT activity was measured with a Transaminase CII-test Wako kit (Wako Pure Chemical, Osaka, Japan).

Histology and TUNEL staining

Liver tissues were fixed in 4% neutralized formalin and embedded in paraffin, then sliced to a thickness of 3 μm. For histological examination, sections were stained with H&E. Apoptotic cells were detected with TUNEL staining using an In Situ Cell Death Detection Kit, POD (Roche, Mannheim, Germany).

Semiquantitative RT-PCR

The total liver RNA for each mouse was isolated using Isogen reagent (Wako Pure Chemical). One microgram of RNA was reverse transcribed with a ReverTra Ace (Toyobo, Osaka, Japan) to obtain cDNA. The primer sequences used in PCR were as follows: LECT2, 5′-ACGTGTGACAGC TATGGCTGTGGACAG-3′ and 5′-AGGTATGCTGTGGGGTCACTGGAG

TC-3'; and GAPDH, 5'-CCCCTGGCCAAGGTCATCCATGACAACTTT-3' and 5'-GGCCATGAGGTCCACCACCCTGTTGCTGTA-3'. Reactions were conducted under the following conditions: precycling at 94°C for 1 min, then 25 cycles consisting of denaturation at 94°C for 30 s, annealing at 55°C for 30 s, and polymerization at 72°C for 1 min.

Quantitative real-time RT-PCR

Quantitative real-time RT-PCR was performed using ABI PRISM 7000 Sequence Detection System (Applied Biosystems, Foster City, CA) according to the manufacturer's protocol. Primers and TaqMan probes specific for TNF-α, IL-4, and FasL were obtained from Assay-on-Demand Gene Expression Products (Applied Biosystems), and IFN-γ was derived from TaqMan Pre-Developed Assay Reagents (Applied Biosystems). For endogenous control, the level of GAPDH in each sample was assayed using TaqMan Rodent GAPDH Control Reagents VIC (Applied Biosystems). Data analyses were performed on ABI PRISM 7000 SDS software version 1.0 (Applied Biosystems).

Statistical analysis

Results were expressed as the mean ± SD. Statistical analyses were conducted using Student's t test or the Mann-Whitney U test. A value of $p < 0.05$ was considered significant.

Results

Generation of LECT2$^{-/-}$ mice

To delete the *lect2* gene, a targeting construct carrying a neomycin cassette was placed within the *lect2* locus in such a way that all exons for this gene were deleted (Fig. 1*A*). Correct targeting of the *lect2* locus was confirmed by PCR and genomic Southern blot analysis (Fig. 1*B*; data not shown). LECT2$^{+/-}$ mice were backcrossed for 10 generations to B6 and intercrossed to generate LECT2$^{-/-}$ mice. Complete loss of LECT2 expression in the liver and serum of LECT2$^{-/-}$ mice was confirmed by RT-PCR and immunoblot analysis, respectively (Fig. 1, *C* and *D*). LECT2$^{-/-}$ mice were born at the Mendelian ratio and were indistinguishable in appearance from wild-type mice. Both male and female LECT2$^{-/-}$ mice were fertile.

Flow cytometric analysis of MNCs from LECT2$^{-/-}$ and wild-type mice

LECT2 is preferentially expressed in the liver (2). LECT2$^{-/-}$ mice exhibited no obvious abnormality in the size or histology of the liver or in serum GPT activity. In addition, the sizes of other tissues, such as spleen and thymus, were normal. We recently reported a possible additional role of LECT2 in Con A-induced hepatic injury (3). Con A-induced hepatitis results from injuries inflicted by various immune cells such as CD4$^+$ T cells and NK1.1$^+$ T cells (8, 14–16). Therefore, we measured the proportions of immune cells in the liver by flow cytometric analysis. Interestingly, we observed that the percentage of hepatic CD3^{int} NK1.1$^+$ cells in LECT2$^{-/-}$ mice was significantly higher than that in wild-

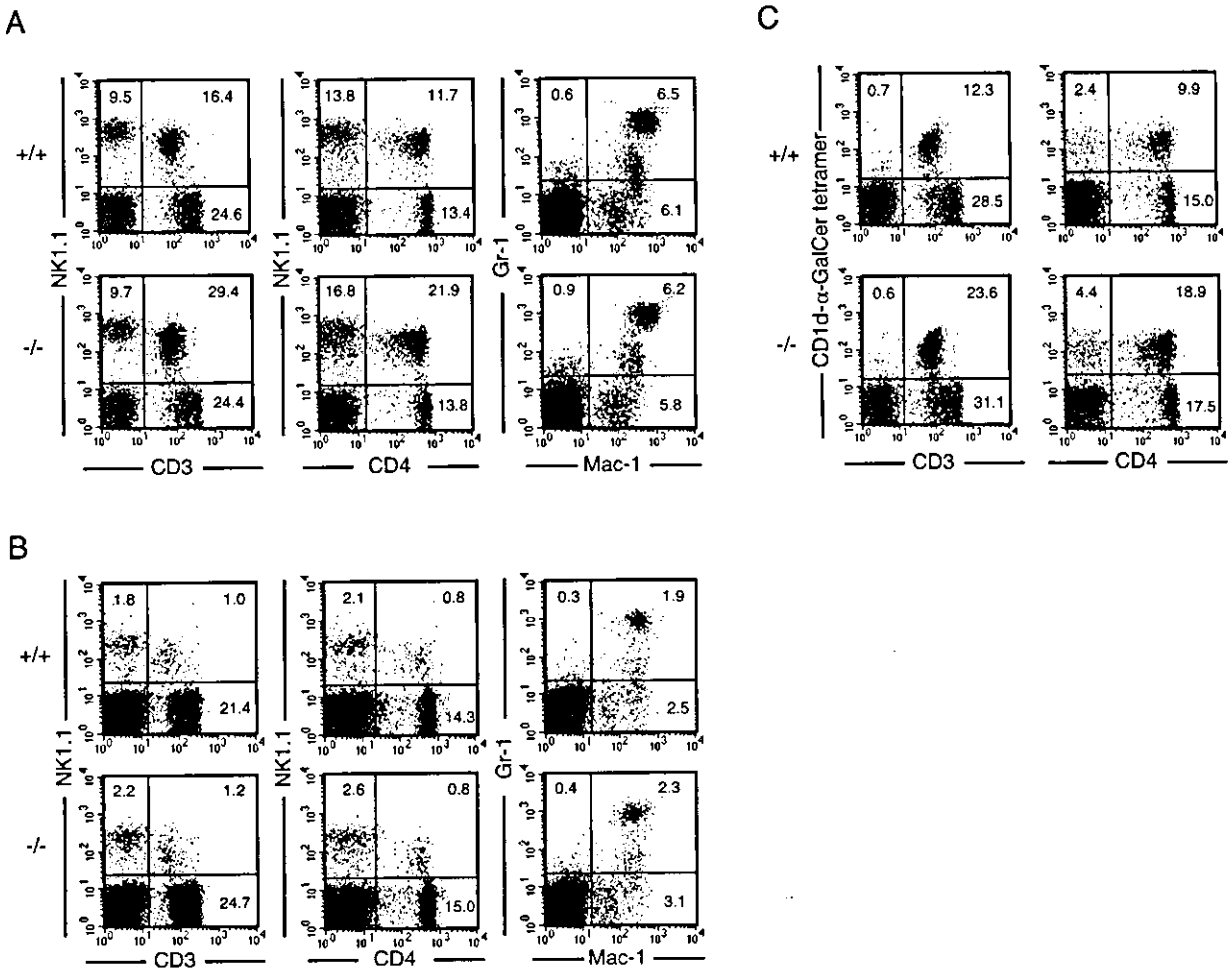

FIGURE 2. Flow cytometric analysis of mononuclear cells in LECT2$^{-/-}$ mice. Two-color staining for CD3 and NK1.1, CD4 and NK1.1, and Mac-1 and Gr-1 against MNCs from the liver (*A*) or the spleen (*B*) was performed. *C*, Hepatic MNCs were stained with CD1d-α-GalCer tetramer and anti-CD3 Ab, and CD1d-α-GalCer tetramer and anti-CD4 Ab. The numbers in the small panels indicate the representative percentages of fluorescence-positive cells in corresponding areas in six mice.

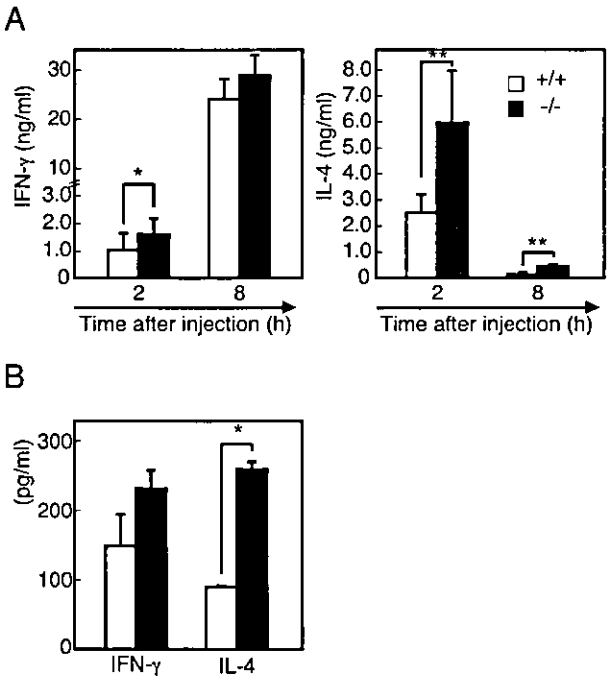

FIGURE 3. Effect of α-GalCer treatment. *A*, IFN-γ and IL-4 expression of mice administered i.p. with α-GalCer (100 μg/kg; $n = 6$ at each time point). *, $p < 0.05$; **, $p < 0.01$. The data are expressed as the mean ± SD. *B*, IFN-γ and IL-4 production by MNCs. MNCs from the liver (2×10^6 cells/ml) were cultured in RPMI 1640 supplemented with 2% FBS. Cytokines released into the culture supernatants were measured 24 h after treatment with α-GalCer (100 ng/ml). The mean values of the results obtained in triplicate are shown with the SD. The data shown are representative of four experiments.

type mice (16.0 ± 4.6% in wild-type vs 26.1 ± 6.2% in LECT2$^{-/-}$; $p < 0.01$; $n = 6$; Fig. 2*A*). The proportion of CD4$^+$ NK1.1$^+$ cells in the livers of LECT2$^{-/-}$ mice also increased compared with that in wild-type mice (11.1 ± 3.5% in wild-type vs 19.3 ± 4.8% in LECT2$^{-/-}$; $p < 0.01$; $n = 6$; Fig. 2*A*). Furthermore, the proportion of CD4$^+$ among the CD3^{int} NK1.1$^+$ cells of LECT2$^{-/-}$ mice was higher than that in wild-type mice (70.1 ± 6.9% in wild-type vs 79.4 ± 1.2% in LECT2$^{-/-}$; $p < 0.01$; $n = 6$). In contrast, there were no differences in the contents of other cell types such as CD3$^+$ NK1.1$^-$ cells (i.e., conventional T cells), CD3$^-$ NK1.1$^+$ cells (i.e., NK cells), or granulocytes (Fig. 2*A*). The total amounts of MNCs obtained from the livers of wild-type and LECT2$^{-/-}$ mice were also comparable ($2.3 \pm 0.4 \times 10^6$ cells in wild-type vs $2.2 \pm 0.7 \times 10^6$ cells in LECT2$^{-/-}$; $n = 6$; Fig. 2*A*). We also examined the proportions of immune cells in spleen, thymus, and bone marrow, but could find no significant differences (Fig. 2*B*; data not shown). These results suggest that LECT2$^{-/-}$ mice contain an increase in the proportion of hepatic NKT cells. The majority of NKT cells express invariant Vα14-Jα18 for TCR that bind to a glycolipid Ag α-GalCer, presented by CD1d. Invariant Vα14 NKT cells can be detected by using CD1d tetramer loaded with α-GalCer (21, 23, 24). LECT2$^{-/-}$ mice contained approximately twice the proportion of CD3^{int} CD1d-α-GalCer tetramer$^+$ (12.2 ± 3.5% in wild-type vs 21.7 ± 3.6% in LECT2$^{-/-}$; $p < 0.01$; $n = 6$) and CD4$^+$ CD1d-α-GalCer tetramer$^+$ cells (9.7 ± 3.0% in wild-type vs 17.7 ± 3.0% in LECT2$^{-/-}$; $p < 0.01$; $n = 6$) in the liver (Fig. 2*C*). We also confirmed by semiquantitative RT-PCR analysis that the expression of Vα14-Jα18 transcripts was definitely high in the livers of LECT2$^{-/-}$ mice (data not shown).

Responsiveness to α-GalCer treatment

NKT cells express high levels of cytokines, especially IFN-γ and IL-4, in specific response to α-GalCer treatment both in vivo and in vitro (25). As previously stated, LECT2$^{-/-}$ mice contain approximately twice the proportion of Vα14 NKT cells that are found in wild-type mice. To address the specific reactivity of NKT cells, we next measured cytokine production after the i.p. administration of α-GalCer to LECT2$^{-/-}$ mice and wild-type mice. Two hours after this treatment, LECT2$^{-/-}$ mice produced a significantly higher level of IL-4 and a slightly increased IFN-γ level compared with wild-type mice (Fig. 3*A*). We also measured the release of IFN-γ and IL-4 from cultured hepatic MNCs after stimulation with α-GalCer. As Fig. 3*B* indicates, higher amounts of IFN-γ and IL-4 were produced from the MNCs of LECT2$^{-/-}$ mice.

Cytotoxicity assay

We next examined two types of cytotoxicity of MNCs prepared from the liver and spleen of wild-type and LECT2$^{-/-}$ mice. NK cell-sensitive cytotoxicity primarily mediated by the perforin-granzyme system was assayed against YAC-1 cells, whereas NKT cell-sensitive cytotoxicity, primarily mediated by the Fas/FasL system, was assayed against syngeneic thymocytes (13, 22, 26–28). Hepatic MNCs from LECT2$^{-/-}$ mice showed substantially greater cytotoxicity against syngeneic thymocytes than did those from wild-type mice (Fig. 4), indicating that the Fas/FasL-mediated cytotoxicity of hepatic MNCs in LECT2$^{-/-}$ mice was much higher than that in wild-type mice. We also observed a slight increase in cytotoxicity in hepatic MNCs from LECT2$^{-/-}$ mice against YAC-1 cells (Fig. 4). The cytotoxicity of splenocytes against syngeneic thymocytes and YAC-1 cells was comparable between wild-type and LECT2$^{-/-}$ mice (Fig. 4).

Con A-induced hepatitis

Growing evidence indicates that NKT cells contribute significantly to the onset of Con A-induced hepatitis by expression of IL-4 and activation of cytotoxic systems (14–16). To examine whether the increase in NKT cells in LECT2$^{-/-}$ mice affects susceptibility to Con A-induced hepatitis, LECT2$^{-/-}$ and wild-type mice were injected i.v. with Con A. Serum GPT activity in LECT2$^{-/-}$ mice was elevated within 5 h after Con A administration compared with that in wild-type mice (Fig. 5*A*). In LECT2$^{-/-}$ mice only, histological examination showed a focal degenerative change, and cell clusters consisting of apoptotic cells could be detected in the liver 5 h after Con A injection (Fig. 5*B*). Con A-induced hepatitis requires the activation of immune cells accompanied by the secretion of various cytokines (13–16, 29). We therefore measured serum

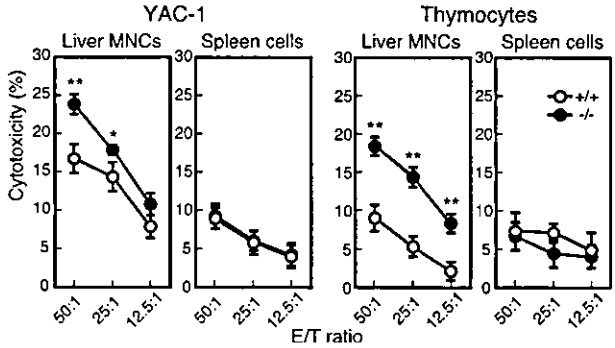

FIGURE 4. Cytotoxicity assays. MNCs were prepared from the liver and spleen of wild-type and LECT2$^{-/-}$ mice. NKT cell-sensitive cytotoxicity was determined using syngeneic B6 thymocytes as target cells. NK cell-sensitive cytotoxicity was determined using YAC-1 cells. Triplicate cultures lasted 4 h at the indicated E:T cell ratio. *, $p < 0.05$; **, $p < 0.01$.